Politecnico di Torino

Master's Degree in Civil Engineering

Tunneling-Induced Settlements in Urban Areas

Academic Year 2024/2025

Supervisor:

Prof. DANIELE MARTINELLI

Co-supervisor:

Eng. VINCENZA FLORIA

Candidate:

HAMID ZEKAVATMAND

Politecnico di Torino

Abstract

Tunneling projects in urban areas are developing rapidly as a result of the growing cities and the demands for modern transportation systems. Due to the lack of space at the surface, underground infrastructures offer a viable solution, but these underground constructions often cause some complex geotechnical challenges. One of the most critical issues is the ground surface settlement induced by tunneling, which puts buildings and utilities located near the project at risk, especially in densely populated areas.

In this thesis, a comprehensive study on tunneling-induced settlement mechanisms in urban areas is provided by examining short-term and long-term ground deformations in both cohesive and cohesionless soils. Both empirical and analytical approaches were explored and compared, including the influential works of Peck, Loganathan & Poulos, and Sagaseta, in order to estimate and control settlements. Additionally, some risk assessment methodologies like Building Condition Surveys (BCS) and Building Risk Assessment (BRA) are introduced and explained in detail. These evaluations aid engineers in assessing the vulnerability of buildings and infrastructure before tunneling excavation, monitoring changes during construction, and guiding mitigation measures in real time.

This study contains some real-world examples to combine theory with detailed case studies. They are used to show the methodology, settlement analysis, vulnerability indexing, and damage classification. Finally, these cases play a crucial role in highlighting the critical need for pre-construction surveys, continuous monitoring, and adaptive construction strategies to reduce settlement risks and increase urban safety.

Politecnico di Torino

Table of Contents

1. Introduction

1.1 Background of Tunneling-Induced Settlements in Urban Areas

In urban areas, in order to support transportation, utilities, and other essential services, more and more subterranean infrastructures are needed, which is why cities have been developing in this way. As a result, we are dealing with fewer surface areas for new constructions, which forces urban planners and engineers to switch to the subsurface for finding solutions to meet the needs for more transportation. Building tunnels has become an effective way to provide transportation systems without interfering with surface-level activities and increasing congestion on the surface. On the one hand, tunneling is a solution to the efficient use of land in crowded areas, especially in megacities. On the other hand, geotechnical challenges such as ground movements and settlements can result from building tunnels. It is important to mention that even slight ground movements can have detrimental effects on densely populated areas where roads and buildings are close to each other, which can lead to structural damage and misalignment of infrastructures and the surrounding environments. However, it is essential to control negative outcomes related to the underground constructions, e.g., settlements, to be safe and reduce the risks [1].

Tunneling-induced settlements usually result from the interactions among structural loads, excavation methods, and soil behavior. When a tunnel is excavated, stress redistribution happens in the surrounding grounds, which often leads to volume loss and next subsidence at the surface [2]. This condition is more critical in soft soils and weak rocks since in these kinds of soils and rocks, the removal of support from the excavated material causes the remaining to collapse. There are various factors that contribute to the structure and extent of settlements, including the tunnel's depth, diameter, excavation technique, and the mechanical properties of the surrounding ground [3]. In shallow tunnels or weak soils, for example, settlements are more likely to be critical and expand over a wider area, but in deeper tunnels that often have more stable ground conditions, surface deformations are generally less critical. In urban areas, tunnels are often located under historical buildings, roads, and other utilities, so even minor settlements can endanger daily life and cause some structural challenges. Therefore, it is essential to consider effective predictive models and active techniques to control ground movements [4].

In order to minimize and control settlements and ensure the stability of surrounding structures and infrastructures, a variety of tunneling techniques have been developed. For instance, Tunnel Boring Machines (TBMs) are widely used in urban areas for tunnel excavation because of their ability to provide continuous support to the excavated face and reduce the probability related to more ground movements. These machines are able to control pressure at the tunnel face and balance groundwater and soil pressures to limit settlement effects. Moreover, the New Austrian Tunneling Method (NATM) is the method that is related to the natural strength of surrounding soil and rock formations. It uses flexible support systems that adapt to the ground conditions. This method is particularly influential in different geological conditions, but needs precise monitoring and adjustments throughout the construction process. Also, a wide range of empirical and analytical methods have been used to estimate settlement in order to decrease ground movement risks. Theses estimations are helpful to provide detailed simulations of soil-structure interactions, which allow engineers to evaluate potential settlement behavior before tunneling process begins.

1.2 Problem Statement

Urban tunneling projects usually deal with important challenges related to ground settlements. Although different predictive models have been proposed and mitigation strategies have been used, uncertainties in subsurface conditions and construction methods make it difficult to achieve precise control for settlements. If ground movements are predicted inappropriately, it can lead to irreversible damages, costly repairs, and even potential safety hazards for surrounding buildings and infrastructures. There is not a completed model that guarantees accurate predictions that can cover different geological conditions, even though empirical, analytical, and numerical methods have been developed to estimate tunnel-induced settlements. Moreover, mitigation activities such as compensation grouting, soil reinforcement, and real-time monitoring require further assessment for their effectiveness. Therefore, the role of the comprehensive study that can integrate theoretical models, real-world case studies, and mitigation techniques is inevitable to improve our understanding related to settlement behavior in urban tunneling projects.

1.3 Research Objectives

The key objective of this research is to understand deeply the mechanisms related to ground movements due to tunneling in urban environments by explaining different types of settlements and assessing theoretical models. The study aims to:

- Investigate the mechanisms of tunnel-induced settlements
    - Analyzing of soil behavior, settlement mechanisms, and influencing factors related to ground movements.
- Prediction models
    - Review of empirical and analytical models used for settlement estimation.
- Assessing the risk of damage for buildings induced by the ground surface settlement
    - Building Condition Survey (BCS): The real condition of the structure are detected before, during and after the excavation.
    - Building Risk Assessment (BRA): To estimate the potential damages related to the expected surface settlement and the vulnerability of the structures.
- Analyzing some real case studies
    - Examining deeply some examples to integrate theoretical aspects with detailed case studies.

1.4 Histories and Cases

1.4.1 TBM

Barcelona Metro Line 9 is a real-world example related to tunneling-induced settlements that occurred during the construction of the tunnel, which is one of the longest urban metro lines in Europe with a length of 47.8 km. This extensive underground metro project is related to tunnel excavation under densely populated urban areas. There were some concerns about the potential settlements because of existing different geological formations, such as soft deposits and soils that influence surrounding structures and infrastructures. Tunnel Boring Machines (TBMs) have been used to minimize ground movements, but some parts tolerated unexpected settlements due to variations in soil conditions and groundwater levels. This example illustrates the importance of proactive engineering solutions to manage tunneling-induced ground movements effectively [5].

1.4.2 NATM

The Munich Metro extension project is another example related to the construction of several underground lines through densely built urban areas. In this project, tunnel diameter is approximately 8–10 meters and tunnel depth is 10–20 meters below ground surface. Ground conditions varied from soft to medium-dense sands in most zones to clay in other areas. In this project, the New Austrian Tunneling Method (NATM) has been chosen to be used since it allowed for adaptive construction based on actual ground behavior, especially in sections where ground conditions were challenging, which was critical in urban areas with sensitive buildings. This method was used with shotcrete initial lining, systematic monitoring of ground deformation, and immediate support adjustments. As a result, real-time monitoring combined with the adaptive philosophy of NATM was critical for providing safe tunneling in this example [6].

2. Ground Movements

2.1 Introduction

Tunnel excavation and construction lead to ground movements, which change the stress condition in the soil and rock surrounding the tunnel. The excavation procedure alters the earth's natural situation, leading the ground to shift toward the excavated area. Some of these movements can be decreased by linings and tunnel supports, but they cannot control all the ground movements because of some limitations in timing and stiffness. As a result, some degree of ground deformations remains, especially when materials compress and the ground deals with the new stress distribution [7].

Settlements surrounding tunnels are usually categorized in three major categories:

2.1.1 Short-term settlements

They happen almost as soon as the tunnel is excavated, owing to the release of in-situ pressures in the soil. These earliest settlements start somewhat forward of the tunnel face, as ground materials shift in reaction to the diminished support. This type of settlement stops once the tunnel's structural support, or lining, is in place and sufficiently reinforced to hold the surrounding ground in place.

2.1.2 Tunnel lining settlements

Due to ground load, tunnel linings may deform slightly, especially in tunnels with large diameters or shallow depths. The weight and pressure from above might cause the liner to compress or shift with time, resulting in modest settlement. This sort of settlement is especially important in tunnels where the ground load is unevenly distributed, as well as in large-diameter tunnels with insufficient depth to evenly distribute stresses.

2.1.3 Long-term settlements

Long-term settlements occur gradually after tunnel construction is completed. These movements can persist for years or even decades and need some consideration in terms of geotechnical engineering in to guarantee

the longevity and stability of structures, especially those built on soft soils. Appropriate modeling, monitoring, and mitigation techniques can manage the risks associated with long-term settlements [8].

2.2 Long-term Settlements in Cohesion less Soils

In these kinds of soils, long-term settlements are mainly caused by water erosion and progressive local instabilities. Cohesion less soils, such as sands and gravels, lack the clay particles that hold moisture and exhibit time-dependent deformation like creep. As a result, long-term ground movements in cohesion less soils are generally minimal and quickly reach completion after loading [9]. However, in some special conditions, such as changes in groundwater levels, loose packing, and repeated loading, these soils may still have settlement in the long run [10]. Cohesion less soils also lack the natural cohesion that makes them vulnerable to movement and volume changes in response to erosion and destabilizing events [11].

2.2.1 Water Erosion

It happens in soils that are not cohesive when running water displaces loose particles, leading to soil loss and collapse of the ground. This process can lead to long-term settlement by slowly reducing soil volume, especially near the surface or around structures, and decreasing foundation or other bearing load elements [12]. When rain or surface water runs across cohesion-free soils, loose particles are transported away, which results in surface-level sediment loss. Over time, the progressive clearance of particles might lead to small and continuous settlements [11]. When water flows under the soil, such as beneath a foundation or near a tunnel, internal erosion or piping might occur. Water seeping through the soil forms small channels that increase during the time, allowing additional particles to be replaced. This condition leads to voids and eventual settlement, particularly if the erosion is continuous or unchecked [13].

2.2.2 Progressive Local Instabilities

Progressive instability refers to local collapses or changes in structure in soil occurring over time. In cohesion less soils, instabilities frequently occur due to cyclic loads, vibration, water flow, and ground disturbance. Unlike cohesive soils, which are capable of bearing some load without shifting, cohesion less soils are less able to resist these forces, resulting in gradual, localized changes in soil structure and long-term settlement [10]. Repeated loading from vehicles, railways, or heavy machinery causes particles in cohesion less soils to gradually rearrange and compact. Minor settlement increments occur over time as the soil compacts under cyclic load [14]. Construction activities such as piling, blasting, and machinery use cause vibrations that can destabilize cohesion less soils. These vibrations interfere with free elements, producing local compaction and small voids that lead to ongoing settlement [9]. When soil particles are disturbed, voids can form, particularly near slopes, embankments, and foundations. These small, isolated holes eventually weaken the surrounding soil, creating settlements as they develop [15].

2.3 Long-term Settlements in Cohesive Soils

Long-term settlements in these soils are caused by the ("primary") consolidation and creep (or "secondary consolidation") that takes place during the time when a load is applied. These settlements need more time, such as months or years, to form, especially in deep or extremely compressible soils like soft clays [16, 17].

There are some influencing factors that affect the magnitude and duration of these settlements:

Soil type: Soft, fine-grained cohesive soils like clays tend to have more settlement because of high water content, low permeability, and high compressibility [9]. In contrast, sandy soils usually have settlements in a shorter period since excess pore pressure dissipates more rapidly.

Load magnitude: The magnitude of loading correlates with the rate and amount of settlement. Heavier

loads accelerate primary consolidation and also increase the secondary consolidation or creep, especially in organic or very soft clays [18].

Over-Consolidation Ratio: OCR is defined as the ratio of the soil's maximum past vertical effective stress to its present vertical effective stress. Lower OCR shows that the soil structure is more deformable under new loading, which leads to greater settlements [19].

Drainage conditions at the tunnel boundary: Drainage conditions significantly impact on the dissipation of excess pore water pressure (EPWP). In saturated soils, the tunnel boundary conditions (impermeable vs permeable) affect the speed related to the dissipation of EPWP, which has effect on the magnitude and rate of settlement. If drainage is limited (e.g., by an impermeable lining), EPWP may take longer, which leads to delaying consolidation and increasing settlement [20].

2.3.1 Consolidation

Primary consolidation in cohesive soils, especially clays, is the process in which soil volume reduces when pore water is drained due to an applied load [17]. This process happens because of excess pore water pressure (EPWP) as a result of a new load, such as the weight of buildings, embankments, and other structures. When a tunnel is excavated in cohesive soils, extra pore water pressure occurs while the soil deals with the new load distribution. When the pressure decreases, the earth consolidates, which leads to gradual compression and settling [21]. This phase of consolidation might take weeks or years, depending on the soil permeability and layer thickness [22]. The rate of primary consolidation is quantified by the coefficient of consolidation (C_V), which depends on the soil's permeability, compressibility, and unit weight [19]. C_V is a critical parameter in determining how quickly a given soil will consolidate under a specific load, and it is often determined by laboratory odometer testing. In tunnel engineering, understanding C_V is essential for assessing the potential post-construction settlements and ensuring safe and durable designs [23].

2.3.2 Creep

Creep, or secondary consolidation, is the gradual settling of the soil after the original consolidation process is finished. This kind of settlement is caused by the long-term compression and reorganization of soil particles rather than by extra pore pressure dissipation [18]. During this process, the soil deforms continuously under a continuous load for a long time even though pore water pressures have fully dissipated. In soft cohesive soils, creep is the progressive, time-dependent deformation produced by continuous applied stress related to tunnel excavation or structural loading [23]. Usually, creep deformation occurs in three stages:

Primary Creep (Transient Creep): It is characterized by a relatively high initial rate of deformation that gradually decreases. This stage represents the time when soil particles are adapting to the applied load, and it often overlaps with the end of primary consolidation.

Secondary Creep (Steady-State Creep): This is the most crucial stage from a geotechnical perspective because the steady rate of deformation can continue for a long time. It can persist for months or years, depending on soil properties and loading conditions [24].

Tertiary Creep: In this last stage, failure results from an acceleration of the rate of deformation. Although this stage is uncommon under normal soil circumstances, it can happen in sensitive soils or under excessive loading [9].

There are some influential factors affecting the creep process:

Soil type: Clayey soils are more likely to creep compared to sandy or gravely soils. They have some minerals like montmorillonite that increase creep potential due to their high compressibility [16].

Stress level: Higher applied stress can lead to higher creep. The soils that experience stresses near their failure limit are more likely to be prone to rapid deformation [17].

Pore water pressure: In undrained conditions, changes in pore water pressure can influence creep. A gradual dissipation of excess pore pressures, which happens in the case of consolidation, can lead to continued deformation [21].

Soil structure and fabric: The arrangement of soil particles and the fabric of the soil play a crucial role in the creep process. Soils with sensitive structures may undergo more significant creep because of their lower structural stability [25].

3. Settlement Estimation

3.1 Introduction

Estimating ground settlement induced by tunneling is an integral part of tunnel research. Also, it is an important aspect of geotechnical design and risk management, especially in urban environments where surface structures and utilities are sensitive to deformation. There are two types of ground deformation: transverse settlement that is across the tunnel axis and longitudinal one that is along the tunnel axis. Both of them are shown in Fig. 1 [26]. Many researches have been done to predict and estimate settlement, which is influential for structural stability and reducing risks for buildings and infrastructures located near tunnels. Different approaches have been proposed to estimate settlement, such as empirical methods based on practical engineering experiences and analytical methods based on theoretical assumption [27].

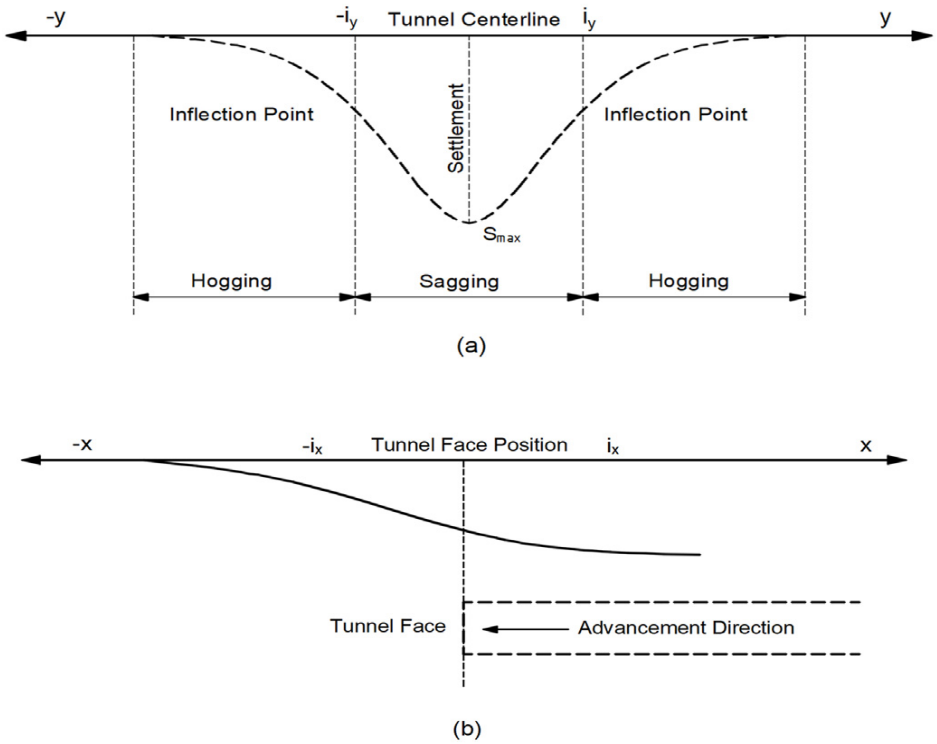

Figure 1. Tunneling-induced ground deformation model. (a) Transverse settlement (b) Longitudinal settlement.

3.2 Empirical Methods

These methods are based on engineering practice and measured field data. They have simple mathematical equations based on measurements gathered from the field. Martos [28] originally proposed that the normal distribution curve can well represent the shape of daily settlement. Then, Peck [29] expanded the research and demonstrated that a Gaussian curve was appropriate for fitting tunneling-induced ground settlement. He analyzed the settlement data from many tunnels and found that the settlement curve was symmetrical above the vertical axis of the tunnel. Finally, he offered the equations for estimating ground surface settlement shown below:

$$S_v = S_{max} \exp\left(\frac{-Y^2}{2\,i^2}\right)$$

$$S_{max} = \frac{V_s}{2.5\,i}$$

$$V_s = V_L \left(\frac{\pi\,D^2}{4}\right)$$

Where S_V is the vertical surface settlement at the Y distance from the tunnel centerline, S_{max} is the maximum ground surface settlement that usually occurs above the tunnel centerline, i is the horizontal distance from the tunnel center to the point of inflection of the settlement (see Fig. 1), Vs is the settlement volume per unit advancement, V_L is the tunnel volume loss, and D is the tunnel diameter.

Based on the hypothesis presented by Peck [29], various methods for calculating S_{max} were proposed. For example, Ranken [30] optimized the relationship between S_{max} and Vs. Additionally, Attewell et al. [31] proposed a new formula to calculate the S_{max} equation.

$$S_{max} = \frac{V_s}{i\sqrt{2\,\pi}}$$

$$S_{max} = \frac{(1+\mu^2)\,P_v}{E}\,\frac{4HR^2}{H^2 - R^2}$$

Where S_{max} is the maximum ground surface settlement, Vs is the settlement volume per unit advancement, H is tunnel depth and R is tunnel radius, X is horizontal distance between pile and tunnel centerline, P_V is vertical component of the principal in situ stress, E is elastic modulus, and μ is Poisson's ratio.

More empirical equations are summarized in Table 1. In addition, the inflection point (i), which determines the shape of settlement trough, may vary in different ground conditions. It is also dependent on tunnel depth and tunnel radius significantly. The empirical equations for estimating inflection point (i) are shown in Table 2.

Table 1. Empirical formulas for predicting tunneling-induced ground settlement.

Empirical Formula	Application Conditions	Reference
$S_{max} = 0.0125\frac{V_L}{i} \times \left(\frac{D}{2}\right)^2$	clay and sand	Schmidt (1969)
$S_{max} = f\left(\frac{H}{2R}\right)$	clay	Attewell and Farmer (1974)
$S_{max} = \frac{V_s}{\sqrt{2\pi} \times i}$	clay and sand	Yoshikoshi et al. (1978)
$S_{max} = \frac{V_s}{\sqrt{2\pi}i}\left[G\left(\frac{x - x_i}{i}\right) - G\left(\frac{x - x_f}{i}\right)\right]$	clay and sand	Attewell and P Woodman (1982)
$S_{max} = 0.785[\gamma_n \times H + \sigma_s] \times \frac{D^2}{i \times E}$	clay and sand	Herzog (1985)
$S_{max} = 4.71[\gamma_n \times H + \sigma_s] \times \frac{D^2}{(3i + d) \times E}$	twin tunnels in clay and sand	Herzog (1985)
$S_{max} = \frac{V_L}{\sqrt{2\pi k(H-h)}} \exp\left[-\left(\frac{x}{\sqrt{2\pi k(H-h)}}\right)^2\right]\ k = \frac{0.175 + 0.325(1 - h/H)}{1 - h/H}$	clay	Mair et al. (1993)
$S_{max} = 0.313\left(\frac{V_L \times D^2}{i}\right)$	clay and sand	Mair and Taylor (1997)
$S_{max} = 4.71[1 - 0.71 \times \exp(-0.018 \times d)] \times (\gamma_n \times H + \sigma_s) \times \frac{D^2}{(3i + d) \times E}$	clay and sand	Hasanpour et al. (2012)
$S_{max} = 0.01875\left(\frac{D^2}{4i}\right) \times e^{0.26[\gamma_n \times H + \sigma_s - \sigma_T]/Cu}$	clay and sand	Chakeri et al. (2013)
$S_{max} = \frac{V_L(1.82 - (H-h)/H)}{1.85 \times \sqrt{2\pi k(H-h)}} \exp\left[-\left(\frac{x}{\sqrt{2k}(H-h)}\right)^2\right]\ k = -\frac{2.8(H-h)}{H} + 2.1$	sand	Wang et al. (2016)
$S_{max} = \frac{V_L\left(\frac{0.5h}{H} + 0.5\right)}{\sqrt{2\pi k(H-h)}} \exp\left[-\left(\frac{x}{\sqrt{2\pi k(H-h)}}\right)^2\right]\ k = \frac{0.44 - (0.28h/H)}{1 - h/H}$	sand	Wang (2021)

S_{max} is the maximum ground surface settlement that usually occurs above tunnel's centerline, Vs is the settlement volume per unit advancement and V_L is tunnel volume loss, i is horizontal distance from tunnel center to point of inflexion of the settlement trough while R and D are tunnel radius and tunnel diameter

respectively. It needs notice that h and H are depth of the calculated settlement trough from the ground surface and tunnel depth respectively. d is distance between tunnel axes, E is elastic modulus, γn is natural unit weight of soil, C_u is undrained cohesion, k is empirical constant of proportionality, σ_s is surface surcharge, σ_T is required face support pressure, x is the longitudinal position of the considered surface point, x_i is the initial position of the tunnel, x_f is the location of the tunnel face, and G is the numerical integration of the normal probability curve. When $x = x_f$, the quantity of G is 0.5, and when $(x - x_i)$ approaches infinity, the quantity of G approaches one.

Table 2. Empirical formulas for the calculation of inflection point.

Settlement Trough (i)	Application Conditions	Reference
$i = H/\left[\sqrt{2\pi} \times \tan\left(\frac{\pi}{4} - \frac{\varphi}{2}\right)\right]$	clay and sand	Peck (1969)
$i = 0.4H + 1.92$	clay and sand	Schmidt (1969)
$i = 0.5H$	clay	Glossop (1978)
$i = R\left(\frac{H}{D}\right)^{0.8}$	clay and sand	Clough and Schmidt (1981)
$i = K \times H$	$K = 0.2 - 0.3$ for sand $K = 0.4 - 0.7$ for clay	O'Reilly and New (1982)
$i = 0.43H + 1.1$	clay	
$i = 0.4H + 0.6$	clay	Herzog (1985)
$i = 0.9\left(\frac{D}{2}\right) \times \left(\frac{H}{D}\right)^{0.88}$	clay and sand	Arioglu (1992)
$i = 0.386H + 2.84$	clay and sand	
$i = 1.392\left(\frac{D}{2}\right) \times \left(\frac{H}{D}\right)^{0.704}$	clay	
$i = \frac{D}{2} \times 1.15\left(\frac{H}{D}\right)^{0.9}$	clay	Loganathan and Poulos (1998)
$i = \frac{H}{D}$	clay and sand	Hamza et al. (1999)
$i = \frac{D}{2} \times \left(\frac{H}{D}\right)^{0.8}$	clay	
$i = 0.74\left(\frac{D}{2}\right) \times \left(\frac{H}{D}\right)^{0.9}$	sand	
$i = 0.63\left(\frac{D}{2}\right) \times \left(\frac{H}{D}\right)^{0.97}$	sand	
$i = 0.29H + R$	clay	Lee (1999)
$i = \frac{1}{3}\left(0.886H + 0.696D \times \left(\frac{H}{D}\right)^{0.704} + 2.84\right)$	clay	Ercelebi et al. (2005)
$i = \frac{1}{4}[0.93H + R \times (0.9\left(\frac{H}{D}\right)^{0.88} + \left(\frac{H}{D}\right)^{0.8}) + 1.1]$	clay and sand	Ercelebi et al. (2011)
$i = \frac{1}{7}[2.116H + R \times (0.9\left(\frac{H}{D}\right)^{0.88} + \left(\frac{H}{D}\right)^{0.8}) + 6.46]$	sand	Chakeri et al. (2013)
$i = 0.56309 \times H - 0.40978 \times D$	sandy cobble strata	Wang et al. (2023)

i is inflection point, R is tunnel radius, D is tunnel diameter, H is tunnel depth, and φ is friction angle of soil [26].

While empirical equations have been a convenient and straightforward methodology for a long time for estimating settlement caused by tunnel construction, they are not applicable in all projects [32] and are mostly suitable for soft ground condition. For different strata conditions, the parameters selection of the empirical formula varies greatly [33]. Moreover, in empirical methods soil parameters are not deemed meaning that the accuracy of the settlement calculated by the empirical method cannot be guaranteed [34]. According to Zhang et al., [35], the variability of predicted results using empirical methods is large. These constraints and limitations show that while empirical methods will continue to be used, they should be combined with other more advanced and comprehensive methodologies.

3.3 Analytical Methods

These methods consider more effective factors and simulate ground responses in a simple manner. They are developed based on fundamental equations of elastic theory, and more emphasis is put on analyzing the interactions between the ground and the tunnel. Sagaseta [36] presented an approach for determining near-ground-surface stress and strain fields induced by point sinks. Based on the assumption that soil material is homogeneous and incompressible, he developed the parameter of ground loss (ε) to predict surface subsidence (Z=0) during tunnel excavation. The formulas are illustrated below:

$$S_x = -\frac{\varepsilon}{2\pi}\frac{x}{H^2+x^2}\left(1+\frac{y}{\sqrt{H^2+x^2+y^2}}\right)$$

$$S_y = \frac{\varepsilon}{2\pi}\left(\frac{1}{\sqrt{H^2+x^2+y^2}}\right)$$

$$S_z = \frac{\varepsilon}{2\pi}\frac{H}{H^2+x^2}\left(1+\frac{y}{\sqrt{H^2+x^2+y^2}}\right)$$

Where H is the tunnel depth, ε is the ground loss, x and y are the coordinates at ground surface, which physically means x is the horizontal distance from the tunnel centerline and y is the distance from the tunnel face

Verruijt and Booker [37] investigated ground surface settlement due to tunnel deformation by employing elastic half-plane theory. They set up two tunnel deformation mechanisms, including a uniform radial displacement (shown in Fig. 2) and an ovalization of the tunnel. Assuming soil is an elastic material, they proposed analytical expressions for calculating the displacements at any point of the half plane. The formulas for calculating vertical and lateral displacement of arbitrary positions are shown below:

$$U_z = -\varepsilon R^2\left(\frac{z_1}{{r_1}^2}+\frac{z_2}{{r_2}^2}\right)+\delta R^2\left(\frac{z_1(kx^2-{z_1}^2)}{{r_1}^4}+\frac{z_2(kx^2-{z_2}^2)}{{r_2}^4}\right)+\frac{2\delta R^2}{m}\left(\frac{z_2(m+1)}{{r_2}^2}-\frac{mz(x^2-{z_2}^2)}{{r_2}^4}\right)-2\delta R^2 H\left(\frac{x^2-{z_2}^2}{{r_2}^4}+\frac{m}{m+1}\frac{2zz_2(3x^2-{z_2}^2)}{{r_2}^6}\right)$$

$$U_x = -\varepsilon R^2\left(\frac{x}{{r_1}^2}+\frac{x}{{r_2}^2}\right)+\delta R^2\left(\frac{x(x^2-kz_1^2)}{{r_1}^4}+\frac{x(x^2-kz_2^2)}{{r_2}^4}\right)-\frac{2\varepsilon R^2 x}{m}\left(\frac{1}{{r_2}^2}-\frac{2mzz_2}{{r_2}^4}\right)-\frac{4\delta R^2 xH}{m+1}\left(\frac{z_2}{{r_2}^4}+\frac{mz(x^2-3z_2^2)}{{r_2}^6}\right)$$

Later, Loganathan and Poulos [38] adapted the approach mentioned above and introduced a new ground loss parameter that incorporates nonlinear ground movement around the tunnel-soil interface (see Fig. 2). With short-term consideration only, they neglect the ground deformation due to tunnel ovalisation (δ=0). Therefore, the optimized formulas are expressed as below:

$$U_{z=0} = 4(1-\mu)R^2\frac{H}{H^2+x^2}\frac{4gR+g^2}{R^2}\exp\left(-\frac{1.38x^2}{(H+R)^2}\right)$$

$$U_x = -xR^2\left(\frac{1}{x^2+(H-z)^2}+\frac{3-4\mu}{x^2+(H+z)^2}-\frac{4z(z+H)}{(x^2+(H+z)^2)^2}\right)\times\frac{4gR+g^2}{4R^2}\exp\{-\left(\frac{1.38x^2}{(H+R)^2}+\frac{0.69z^2}{H^2}\right)\}$$

Where ε is the uniform radial ground loss, δ is the long-term ground deformation due to ovalization of the tunnel, g is the gap parameter, $z_1 = z - H$, $z_2 = z + H$, $r_1^2 = x^2 + z_1^2$ 1, $r_2^2 = x^2 + z_2^2$, R is the tunnel radius, H is the tunnel depth, $m = 1 / (1 - 2\mu)$, $k = \mu (1 - \mu)$, and μ is the soil Poisson's ratio.

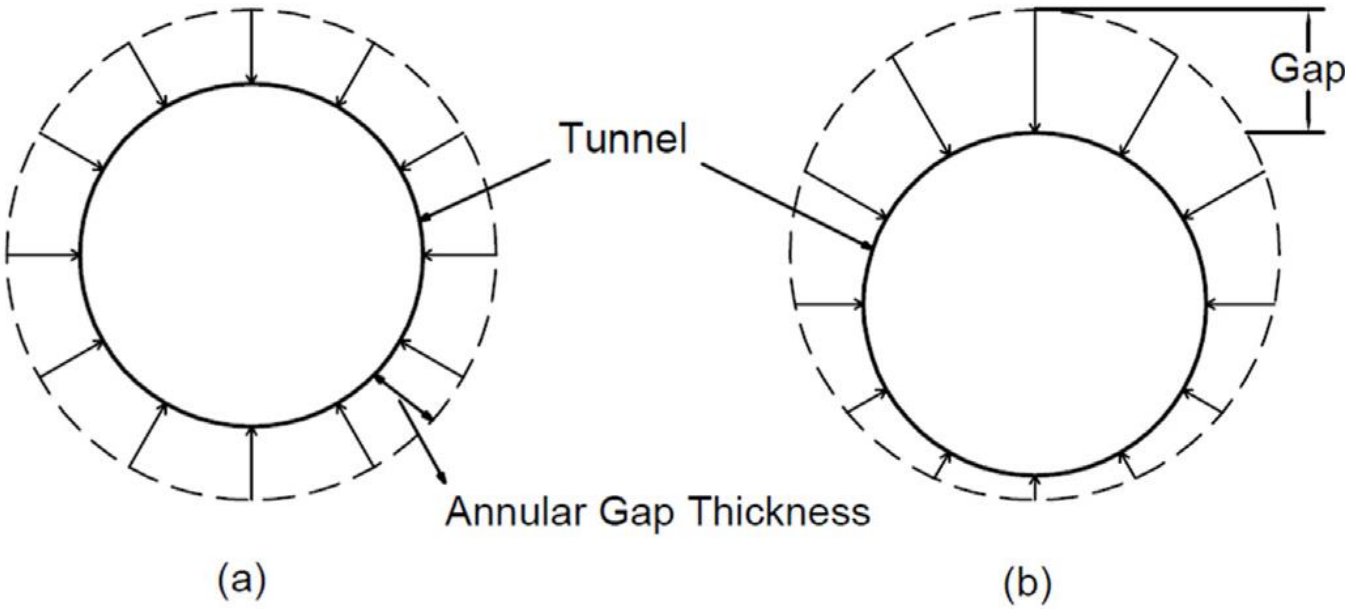

Figure 2. Circular ground deformation patterns around section. (a) Uniform contraction [37] (b) Uniform contraction with vertical displacement [38].

Similarly, Gonzaíez and Sagaseta [39] improved the mentioned analytical equations by considering soil volumetric compressibility. They clarified that the total deformation of the tunnel is caused by three parts: ground loss, ovalisation and vertical movement of the tunnel itself, shown in (Fig. 3), and the general equations for analyzing ground movement at the surface are demonstrated below:

$$S_{z=0} = 2\varepsilon R\left(\frac{R}{H}\right)^{2\alpha-1} \times \frac{1}{\left(1+x'^2\right)^{\alpha}}\left(1+\rho\frac{1-x'^2}{1+x'^2}\right)$$

$$S_x = -2\varepsilon R\left(\frac{R}{H}\right)^{2\alpha-1} \times \frac{x'}{\left(1+x'^2\right)^{\alpha}}\left(1+\rho\frac{1-x'^2}{1+x'^2}\right)$$

Where H is tunnel depth, R is tunnel radius, u is uniform radial displacement, α is the exponent for volumetric compressibility, ε is radial contraction (u/R), δ represents ovalisation, ρ is relative ovalisation δ /ε, and the prime (′) means the magnitudes are scaled by tunnel depth.

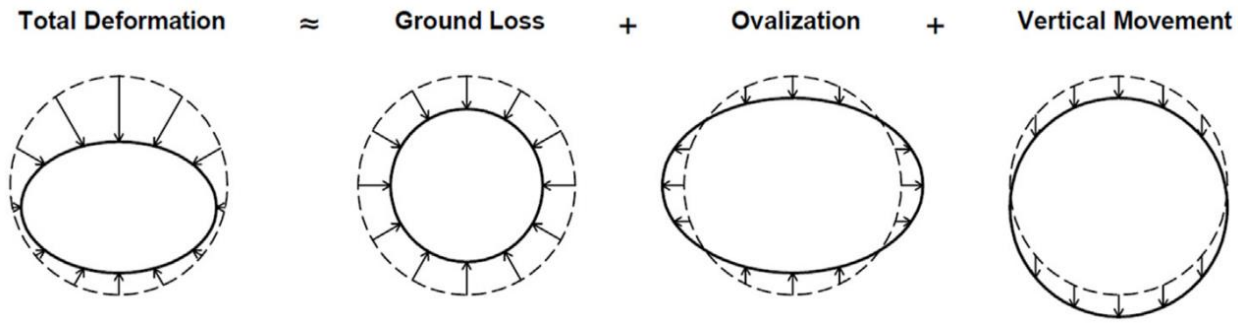

Figure 3. Components of tunnel deformation illustrated by Gonzaíez and Sagaseta [39].

Three are other formulas that are summarized and shown in the Table 3 in the next page.

Table 3. Analytical formulas for predicting tunneling-induced ground settlement.

Analytical Formula	Application Conditions	Reference
$S(x) = \frac{1}{\sqrt{2\pi}i} VL \exp\left(-\frac{x^2}{2i^2}\right)$	Homogeneous soil, Gaussian curve	Peck (1969)
$S(x) = \frac{VL}{\sqrt{2\pi}i} \cdot \exp\left(-\frac{x^2}{2i^2}\right)$	Homogeneous soil	O'Reilly and New (1982)
$S(x) = \frac{q \cdot B}{E_s} \cdot I_z$	Clay and sand	Mair et al. (1993)
$S(x) = \frac{1}{2\pi} \cdot \frac{q \cdot D}{H} \cdot \exp\left(-\frac{x^2}{2i^2}\right)$	Tunneling in clay and sand	Loganathan and Poulos (1998)
$S(x) = VL \cdot \frac{\sqrt{\pi}D}{4H} \cdot \left[1 - \exp\left(-\frac{2H^2}{D^2}\right)\right]$	Circular tunnels in sand	Verruijt and Booker (1996)
$S(x) = \frac{VL}{\sqrt{2\pi k(H-h)}} \exp\left(-\frac{x^2}{2k(H-h)}\right)$	Clay and sand	Mair and Taylor (1997)
$S(x) = \frac{VL}{2\pi} \int_{-i}^{i} \exp\left(-\frac{x^2}{2}\right) dx$	Homogeneous soil, Gaussian-based	Attewell and Woodman (1982)
$S = 4.71 \cdot \gamma_n \cdot \frac{H \cdot D^2}{(3i+d) \cdot E} \cdot \exp(-kx)$	Clay and sand	Hasanpour et al. (2012)
$S = \frac{0.01875 \cdot (D^2)}{4i} \cdot e^{0.26[\gamma_n H + \sigma_5 - \sigma_7]/c_u}$	Clay and sand	Chakeri et al. (2013)
$S(x) = \frac{VL(1.82-(H-h)/H)}{1.85\sqrt{2k(H-h)}} \cdot \exp\left(-\frac{x}{2k(H-h)}\right)$	Sandy soils	Wang et al. (2016)
$S(x) = \frac{VL(0.5h/H+0.5)}{\sqrt{2\pi k(H-h)}} \cdot \exp\left(-\frac{x^2}{2k(H-h)}\right)$	Clay and sand	Wang et al. (2021)
$S = \frac{\gamma \cdot H}{E_s} \cdot \ln\left(\frac{\sigma_f}{\sigma_0}\right)$	Consolidation settlement in clay	Asaoka (1992)
$S = C \cdot \frac{q \cdot D}{\sqrt{E}} \cdot \exp(-\alpha x)$	Generalized soft clay	Lee et al. (2001)
$S = \frac{VL}{2\pi i} \cdot \exp\left(-\frac{x^2}{2i^2}\right) + K \cdot D$	Twin tunnels in clay	Ng et al. (2004)
$S = 0.785[\gamma \cdot H + \sigma_5] \cdot \frac{D^2}{i \cdot E}$	Tunneling in soft clays	Mair and Taylor (1997)

4. Predicting Risk of Damage to Buildings and Utilities

4.1 Introduction

Ground movements resulting from tunneling in urban areas influence buildings, utilities, and other surrounding structures. As a result, some issues, including cracking, tilting, loss of serviceability, and even structural failure, can result from ground movements. To minimize risks and damages, systematic procedures have been developed for predicting and assessing potential damage. The process related to assessing the risk of damage for buildings induced by the ground surface settlement caused by the tunnel excavation is based on two analyses [7]:

1. The Building Condition Survey (BCS): to verify the actual state of buildings before, during, and after tunnel construction.

2. The Building Risk Assessment (BRA): to consider the potentially expected damages based on settlement predictions and the intrinsic vulnerability of the structures.

The overall procedure is shown in Fig. 4, and has the following anticipated steps:

- Recognize the "control parameters," the parameters that affect how a building reacts to settlements (Fig. 5). [$S_{max:}$ maximum vertical settlement, $\Delta S_{max:}$ max differential or relative settlement, $\alpha_{max:}$ maximum angular strain (sagging when positive; hogging when negative), $\beta_{max:}$ maximum angular distortion, ω: tilt (rigid body rotation of the whole superstructure or a well-defined part of it), Δ_{max}: maximum relative deflection (maximum displacement relative to the straight line connecting two reference points with a distance L)].
- With regard to the values assumed by the "control parameters," determine the general standards for setting limitations for the settlement and heave as functions of the particular damage classification system used for the project.
- Undertake the general ground movement prediction (greenfield movements) in order to identify the "construction zone of influence" (also known as the "control zone"), within

which buildings must be inspected to assess the risk of damage (e.g., all buildings within the contours of 1/750 angular distortion and 5 mm settlement, or all buildings at a specific distance on each side of the tunnel alignment).

- For every building that has been identified as being within the "control zone," conduct a settlement sensitivity analysis (i.e., evaluate each building's condition in relation to the amount of ground movement it can withstand before any visible damage begins to appear) and establish the tolerance levels for the maximum amounts of settlement, angular distortion, or deformations.
- Sort all the detected buildings into various risk groups by comparing the settlement forecasts with the settlement sensitivity analysis's findings.
- In order to record the anticipated ground movements and the reaction of nearby buildings and services, prepare a Ground Movement Analysis Report taking into account the following factors: the ground conditions, the structure's arrangement, the kind of nearby structures and utilities, and the construction process.
- Identify the buildings that need to be protected and that are at risk.
- Determine which structures need to be surveyed and given extra attention while they are being built.
- Specify the approach for managing settlement risk.
- Store and preserve all pertinent building data for usage by all stakeholders in a dynamic, relational GIS database.

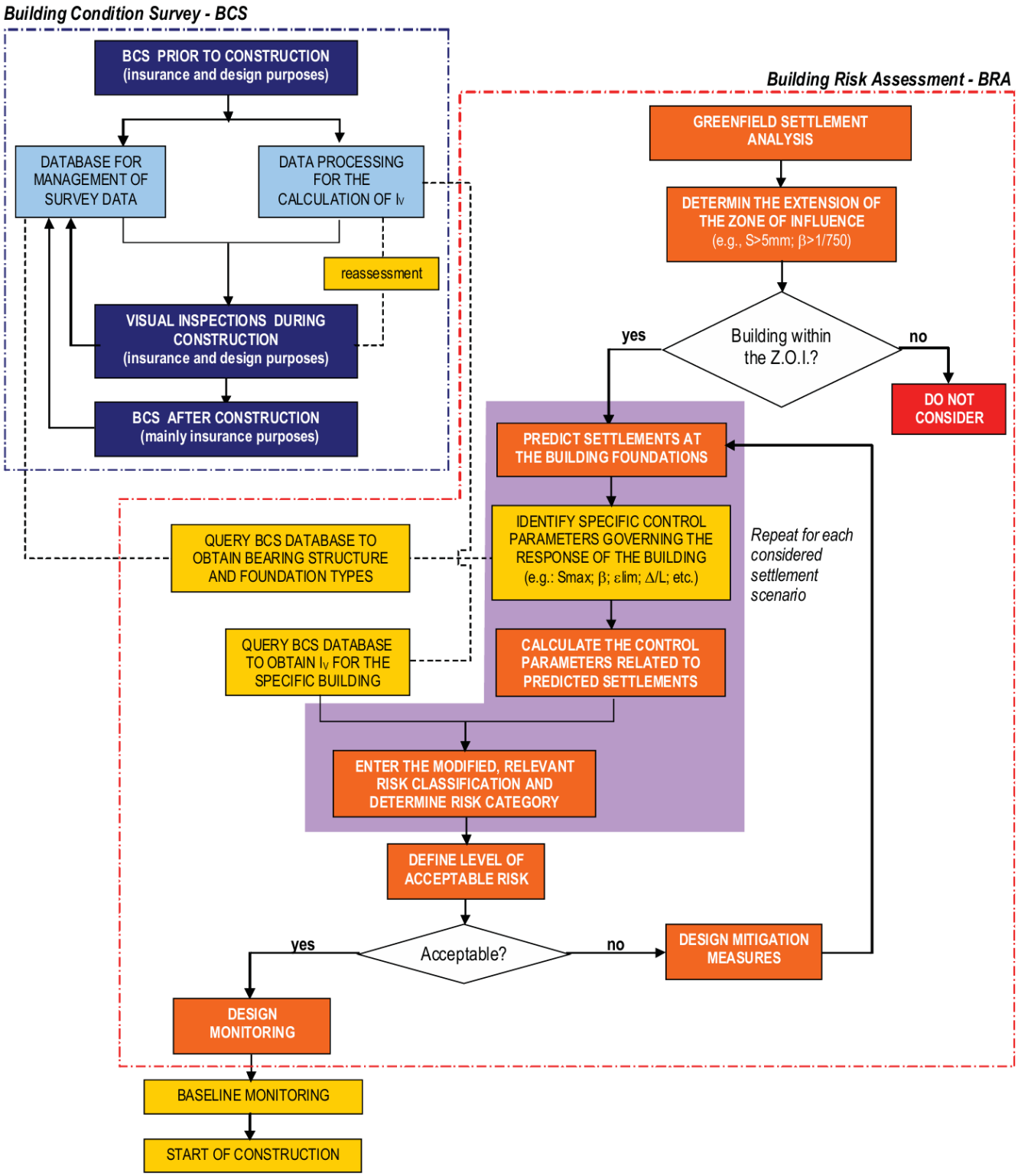

Figure 4. Schematic flowchart of BCS and BRA [7].

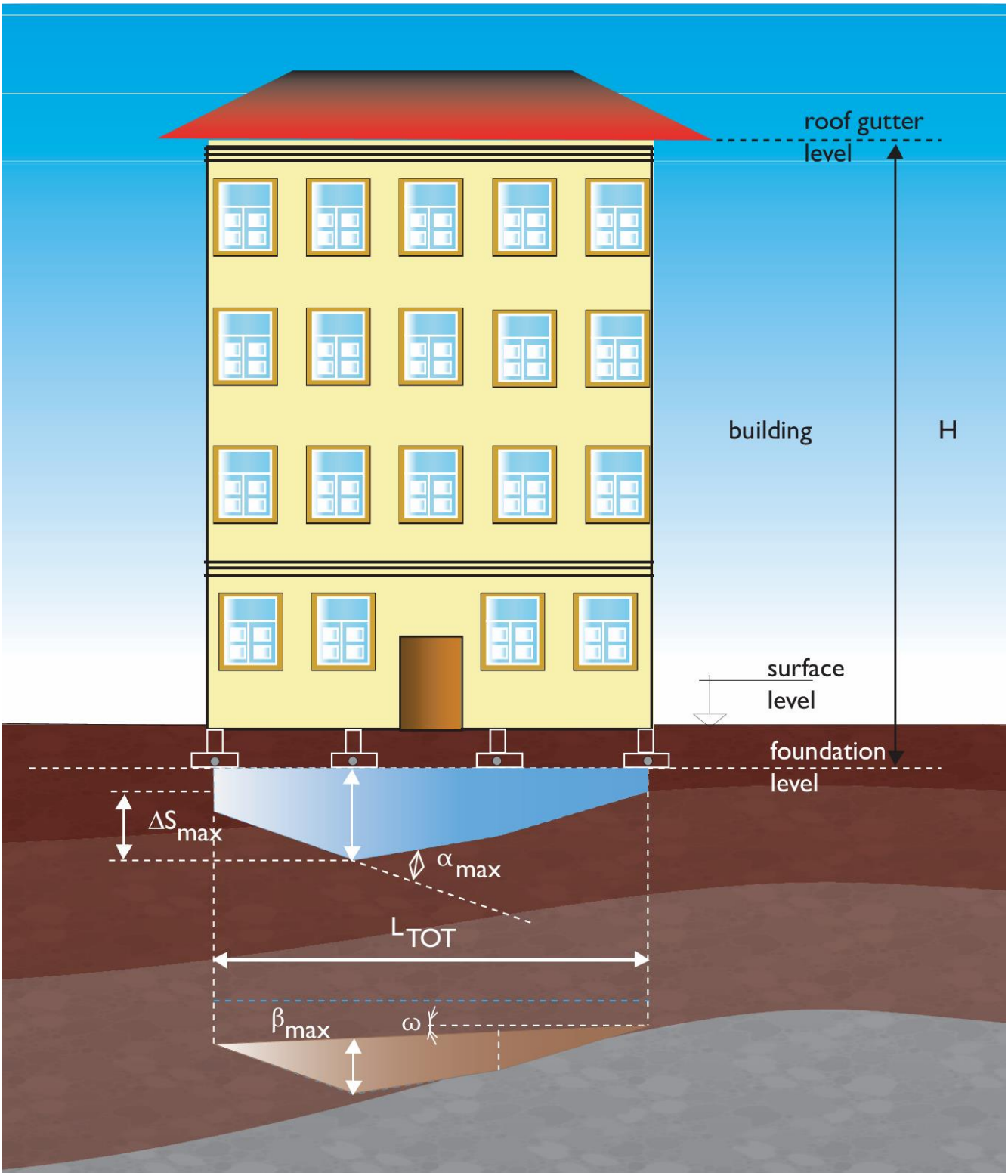

Figure 5. Control parameters that regulate the behavior of a building towards settlements [7, 40].

4.2 Building Condition Survey (BCS)

The condition surveying of all structures and certain inspectable utilities inside the zone of impact of the subterranean construction activities must include three separate stages of surveys to map defects, namely, prior to construction, during construction, and post-construction surveys. Regardless of whether damage is anticipated or has already happened, it is best practice to document the state of every structure inside the control zone for the benefit of all parties concerned.

Moreover, an accurate Building Condition Survey (BCS) is essential to address various possible claims related to property owners. BCS gathers historical building data and creates a map of building defects that will be used to evaluate the structure's vulnerability before it is constructed. A team of qualified structural engineers who will carry out the work on site should create specifications and methods for the BCS surveys, as well as forms for the organized, consistent, and coherent collecting of data. Every building will have its reference number, which is essential for managing and communicating information about every property, facilitating the management of data through a database [7].

In the prior-to-construction stage of survey, the activities done for every single building will have the following aspects:

- A study is conducted to gather data including: the building's age, the project plans, the foundation type and depth, the number of stories, bearing structure type, history of prior repairs, and addition of more stories. Also, the study finds out weather the building is listed as part of historic or architectural heritage, which would make it a particularly sensitive structure.

- A visual examination of the building's conditions: every visible components is inspected and reported in terms of use, verticality and crack detection, a list of flaws, and photographic documentation. When evaluating a building, it is common to examine the roof and the basement as well as a few intermediary floors for a high-risk building. In certain cases, examining the type and state of the foundations will be preferable.

The inspected buildings' level of vulnerability will be evaluated using the results of the pre-construction BCS. Vulnerability is an inherent feature of a building, which depends on the building's history and shows how distant it is from being in ideal condition. The higher the vulnerability, the lower its tolerance towards additional, induced deformation before displaying a particular kind of damage. The vulnerability can be expressed using a so-called Vulnerability Index I_V [41, 42], which is produced by applying engineering judgment to analyze the data gathered during the BCS. The vulnerability index ranges from 1 to 100, and it is categorized into five categorizes, as shown in Table 4 below, where buildings in good condition will undergo any damage or have an extremely low value.

Table 4 Vulnerability Index

Vulnerability Index I_V	Type of vulnerability
0 - 20	Negligible
20 - 40	Low
40 - 60	Slight
60 - 80	Moderate
80 - 100	High

Also, an example of calculation of the vulnerability index is demonstrated in the next page Table 5.

Table 5. Example of calculation of vulnerability Index [7].

PROJECT NAME			Building code		PAGE
CALCULATION OF THE VULNERABILITY INDEX Chiriotti et al., 2001)			0001		1/2
Maxium value: 25	A. STRUCTURAL BEHAVIOUR OF THE BUILDING				
	Characteristic		*Index*	*Assumed value*	
	A.1. Horizontal structural elements				
	A.1.1. Wood structure		6	6	x
	A.1.2. Reinfor ced concrete		0		
	A.1.3. Mixed structure		3		
	A.2. Vertical structural elements				
	A.2.1. Masonry elements		6	6	x
	A.2.2. Steel elements		0		
	A.2.3. Reinforced concrete elements		3		
	A.2.4. Mixed elements		4		
	A.3. Foundations - source of information				
	A.3.1. Direct (drawings, contractor)		0		
	A.3.2. Indirect (property owner, inhabitants, for similarity with known structures, assessed)		4	4	x
	A.4. Type of refurbishment, if any				
	A.4.1. Unknown		2		
	A.4.2. Increasing opening in the façade (or bearing walls)	6			
	A.4.3. Modifications maintaining the construction method		0		
	A.4.4. Modifications improving the construction method	3			
	A.4.5. Consolidation (bearing structure or foundations)		5		
	A.4.6. Adding floors	4		4	x
	A.4.7. Small interior works		0		
	State of the refurbishment works (*)				
	A.4.a. Done or in progress	1	0	x	
	A.4.b. Designed	0	1		
	A.5. Presence of basement levels				
	A.5.1. No		0		
	A.5.2. Yes		3	3	x
				PARTIAL TOTAL A.	**23**

4.3 Building Risk Assessment (BRA)

The BRA is the process in which the building's condition, including structural elements, building systems, and safety situations, is assessed. Also, visual examinations would be necessary to find any defects or possible risks that may endanger the safety of the inhabitants or property. With regard to the identification of risks and vulnerabilities, risks and their possible outcomes are evaluated as part of the BRA process. Then, based on the results of the risk assessment, suggestions and methods for risk mitigation are created in order to improve the building's overall resilience and safety [7].

It is important to classify damage that a structure can undergo in order to provide a precise damage categorization for buildings. The following are the three commonly used damage classifications:

- *Aesthetic* damages are mostly related to the inside walls and their finishes and are associated with minor structural cracks. These damages are easily fixed, and in general, a simple redesign is sufficient to cover the light cracks.
- *Functional* damages refer to the loss of use or functionality of building components (such as stuck doors and windows and damaged pipelines) or of sensitive equipment placed inside the building (like precision instruments that are sensitive to differential movements); the building's structural integrity is unaffected, but the lack of serviceability can have economic and commercial effects on the building and the activities it hosts.
- *Structural* damage that results from severe deformations or cracks in the supporting structures might cause the building to collapse completely or partially. These damages may occasionally stay partially undetected beneath the finishes. However, plaster and whitewash are reliable markers of the spread of cracks.

The damage classifications found in technical literature are based on the kind of damage as well as the range of values that specific control parameters assume as a result of movements that external sources such as tunneling produce in structures. Different control parameters are used by damage classifications based on the particular types of structures they pertain to.

Burland [40] proposed the damage classification (see Table 6) based on the deflection ratio Δ_{max}/L that is related to maximum tensile strain ε_{max} (shown in Fig.7a). This classification is useful for masonry structures and shallow spread foundations. It is crucial to mention that although ε_{max} is the main control parameter, a parallel control has to be performed on the maximum settlement at the level of the building foundations, which should be kept below 250–350 mm (corresponding to building quality) in order to prevent damages related to the serviceability of the building [7].

Table 6. Damage classification established by Burland [40].

Category of risk of damage	*Degree of severity*	*Description of typical damage*	*Crack width [mm]*	*Control parameter (tensile strain) ε_{lim} [%]*
0 aesthetic	Negligible	Hairline cracks	<0.1	0–0.05
1 aesthetic	Very slight	Fine cracks which are easily treated during normal decoration. Damage generally restricted to internal wall finishes. Close inspection may reveal some cracks in external brickwork or masonry.	<1.0	0.05–0.075
2 aesthetic	Slight	Cracks easily filled. Redecoration probably required. Recurrent cracks can be masked by suitable linings. Cracks can be visible externally and some repointing may be required to ensure watertightness. Doors and windows may stick slightly.	<5.0	0.075–0.15
3 aesthetic/ functional	Moderate	The cracks require some opening up and can be patched by a mason. Repointing of external brickwork and possibly a small amount of brickwork to be replaced. Doors and windows sticking. Service pipes may fracture. Watertightness often impaired.	5–15 (many crack with width >3 mm)	0.15– 0.3
4 functional/ serviceability	Severe	Extensive repair work involving breaking-out and replacing sections of walls, especially over doors and windows. Windows and door frames distorted, floor sloping noticeably. Walls leaning or bulging noticeably, some lose of bearing in beams. Service pipes disrupted.	15–25 (but depend on the number of cracks)	>0.3
5 structural	Very severe	Major repair job involving partial or complete rebuilding. Beams lose bearing, walls lean badly and require shoring. Windows broken with distortion. Danger of instability.	>25 (but depend on the number of cracks)	

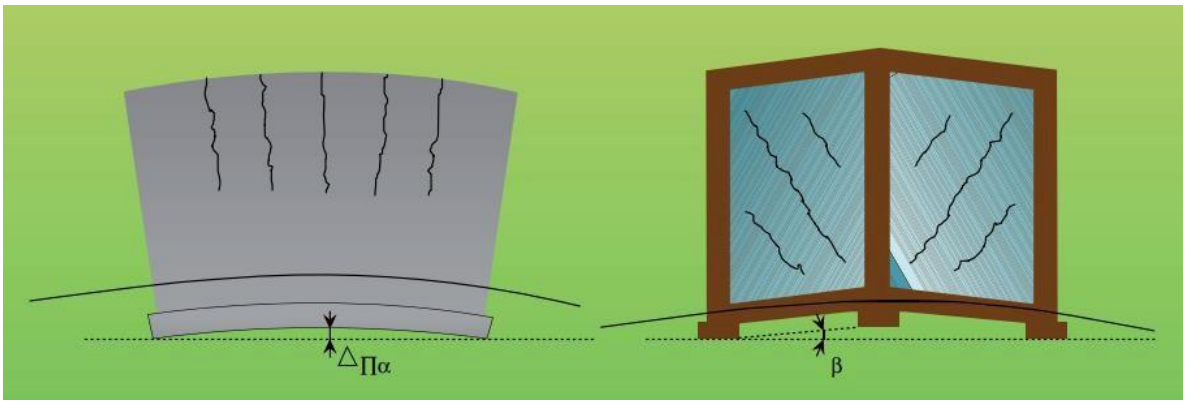

Figure 7. Probable behavior of different kind of bearing structures undergoing a "hogging mode" type of induced deformations: (a) masonry and (b) framed buildings [7].

Moreover, Rankin [43] proposed the damage classification (see Table 7) related to frame building with isolated foundations or with pile foundations in which the distance among piles is such that the "bearing group effect" is not triggered. Damage is related to the differential settlements among the isolated foundations, and in this case, the angular distortion β becomes the most relevant control parameter that is also accompanied by the maximum settlement S_{max} (Fig. 7b).

Table 7. Damage classification established by Rankin [43].

Category of risk of damage	*Degree of severity*	*Description of typical damage*	*Control parameters*	
			β_{max}	S_{max} *[mm]*
1 aesthetic	Negligible	Superficial damage unlikely.	<1/500	<10
2 aesthetic	Slight	Possible superficial damage which is unlikely to have structural significance.	1/500–1/200	10–50
3 functional	Moderate	Expected superficial damage to buildings and expected damage to rigid pipelines.	1/200–1/50	50–75
4 serviceability and structural	High	Expected structural damage to buildings and damage to rigid pipelines; possible damage to other pipelines.	>1/50	>75

It is important to highlight that both above-mentioned classifications are valid for good-condition buildings, but if a structure is already damaged, some correction factors need to be introduced. Chiriotti et al. [41, 42] adjusted Burland and Rankin thresholds by considering the vulnerability index. These new values are more tough and cautious from the point of view of safety. Table 8 and Table 9 show the new thresholds for Burland and Rankin, respectively.

Table 8. New Burland damage classification

Category of damage	*Vulnerability index I_V of the building*									
	Negligible		*Low*		*Slight*		*Medium*		*High*	
	$0 < I_V < 20$		$20 < I_V < 40$		$40 < I_V < 60$		$60 < I_V < 80$		$80 < I_V < 100$	
	Reduction factor F_R									
	$F_R = 1.0$		$F_R = 1.25$		$F_R = 1.50$		$F_R = 1.75$		$F_R = 2.0$	
	Control parameter									
	ε_{lim} [%]		ε_{lim} [%]		ε_{lim} [%]		ε_{lim} [%]		ε_{lim} [%]	
	min.	max.	min.	max.	min.	max.	min.	max.	min.	max.
0	0,000	0,050	0,000	0,040	0,000	0,033	0,000	0,029	0,000	0,025
1	0,050	0,075	0,040	0,060	0,033	0,050	0,029	0,043	0,025	0,038
2	0,075	0,150	0,060	0,120	0,050	0,100	0,043	0,860	0,038	0,075
3	0,150	0,300	0,120	0,240	0,100	0,200	0,860	0,171	0,075	0,150
4 to 5	>0,300		>0,240		>0,200		>0,171		>0,150	

Table 9. New Rankin damage classification

Category of damage	*Vulnerability index I_V of the building*									
	Negligible		*Low*		*Slight*		*Medium*		*High*	
	$0 < I_V < 20$		$20 < I_V < 40$		$40 < I_V < 60$		$60 < I_V < 80$		$80 < I_V < 100$	
	Reduction factor F_R									
	$F_R = 1.0$		$F_R = 1.25$		$F_R = 1.50$		$F_R = 1.75$		$F_R = 2.0$	
	Control parameter									
	S_{max} [mm]	β_{max}	S_{max} [mm]	β_{max}	S_{max} [mm]	β_{max}	S_{max} [mm]	β_{max}	S_{max} [mm]	β_{max}
1	<10	<1/500	<8	<1/625	<6,7	<1/750	<5,7	<1/875	<5	<1/1000
2	10–50	1/500–1/200	8–40	1/625–1/250	6,7–33	1/750–1/300	5,7–28,5	1/875–1/350	5–25	1/1000–1/400
3	50–75	1/200–1/50	40–60	1/250–1/63	33–50	1/300–1/75	28,5–43	1/350–1/88	25–37,5	1/400–1/100
4	>75	>1/50	>60	>1/63	>50	>1/75	>43	>1/88	>37,5	>1/100

When the vulnerability index and the damage category are defined, a risk matrix can be built, as shown in Fig. 8. On the x-axis the damage category is located, and on the y-axis the vulnerability index is placed. Therefore, by combining these two pieces of information, it is possible to define the risk related to each building expressed by a color:

- Green: the potential damage is negligible or slight, and the building is in good condition.
- Yellow: the induced damage to the building is negligible or slight, but due to its condition, standard monitoring is needed during the excavation.
- Orange: the effects of the excavation on the building could induce damage, so a detailed monitoring program must be selected.
- Red: the risk is high because of the amount of the induced deformation; hence, in addition to the detailed monitoring system, ground improvement treatments should be designed.

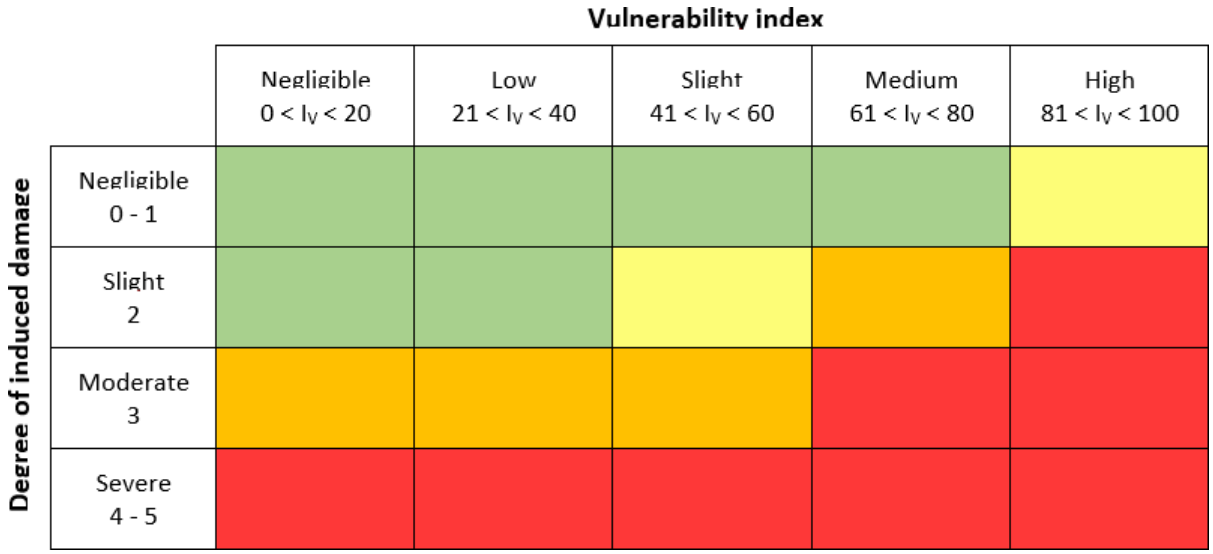

Figure 8. Risk Matrix

4.4 Real Case Study
4.4.1 Introduction

The Elizabeth Line, which crosses London from west to east, is one of the most ambitious infrastructure projects in Europe. The length of this project is 21 km of twin-bored tunnels constructed under central London with eight new stations built on this section of the line (Fig. 9). A key requirement of the project was to keep the character of Denmark Street and maintain the independent shops trading before, during, and after the development. For this reason, the development was split into two parts: the new buildings and basement construction in the north and west of the site, known as 'Zone 1,' and the retained and refurbished buildings on Denmark Street and St Giles High Street, known as 'Zone 2' (Fig. 10). Due to excavation beneath historic buildings, high groundwater levels, and dense urban infrastructure, the assessment of building damage placed near the project was inevitable [44].

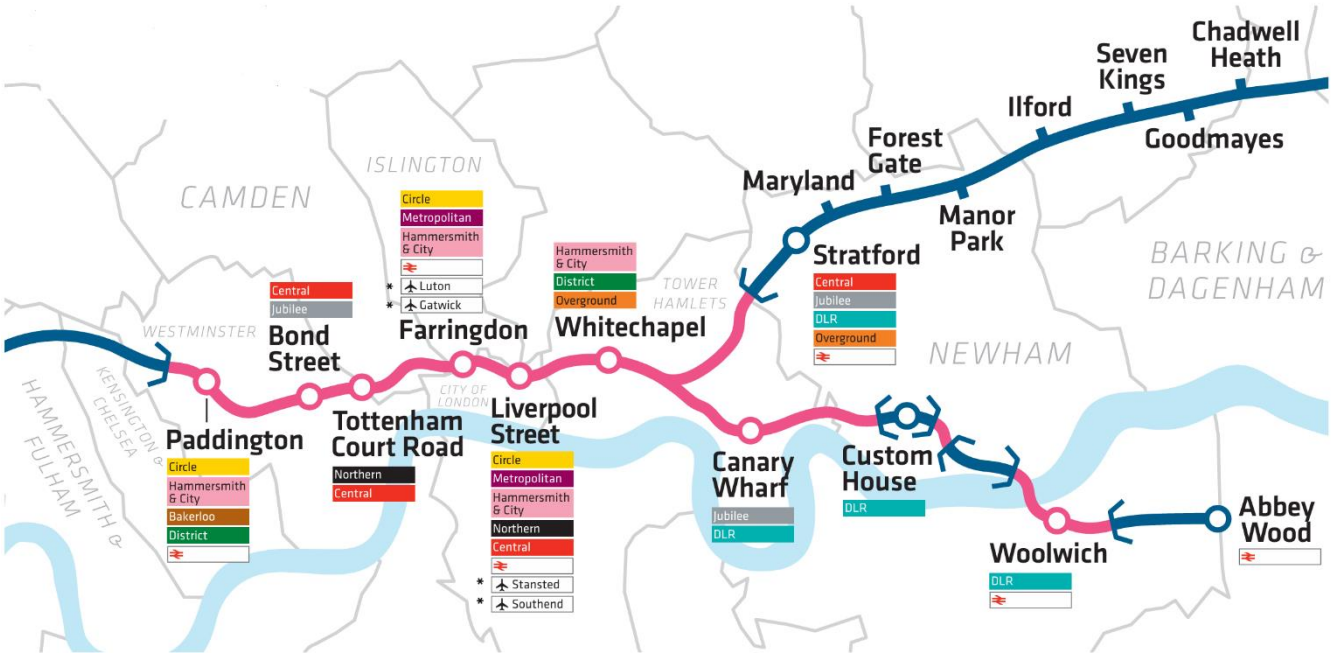

Figure 9. Central London section of Elizabeth line [44] (bored tunnels and new underground stations shown in red).

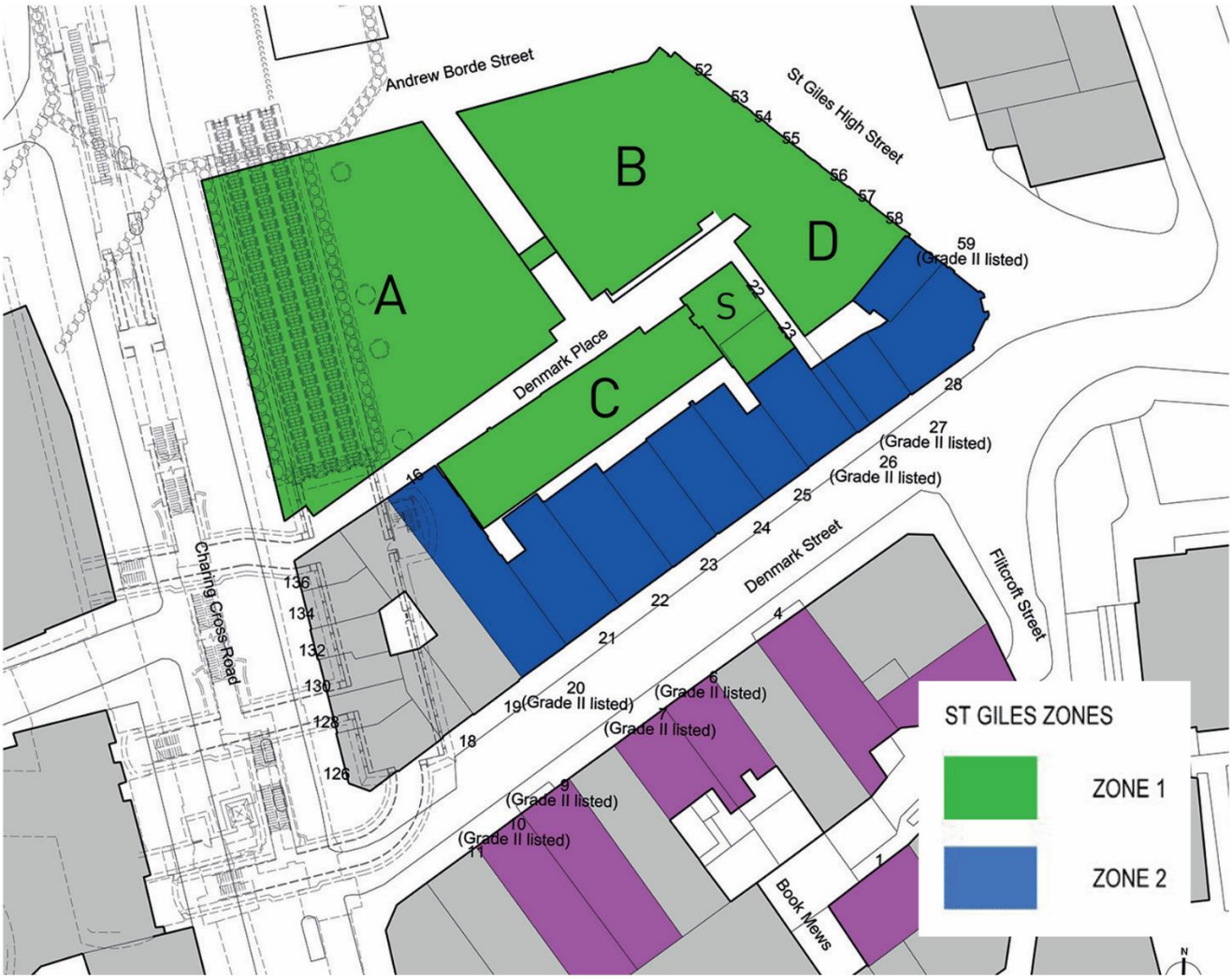

Figure 10. Site plan with listed buildings and extent of Zone 1 and Zone 2.

4.4.2 Selection and Evaluation of Buildings

Before starting the construction, some surveys related to structures' situation were carried out to evaluate the condition of buildings located around the proposed route. The first stage of the BCS is to define the Zone of Influence (ZOI), an area adjacent to the metro line where the buildings to be examined fall. In this project, ZOI was defined as 30 meters from tunnel alignment, which is approximately 5 times the tunnel diameter, and considering buildings alone, there were about 4000 buildings along the route, of which around 300 were listed. This process covered assets including both low-rise masonry structures on shallow foundations and taller, framed structures on piled foundations, and other structures and statutory services.

4.4.3 Classification and Assessment of Building Damage

For all assets placed within the zone of influence that might be affected by the works, the damage assessment process was carried out by assuming that buildings behaved as elastic beams and moved as per greenfield ground movements (Fig. 11) [44].

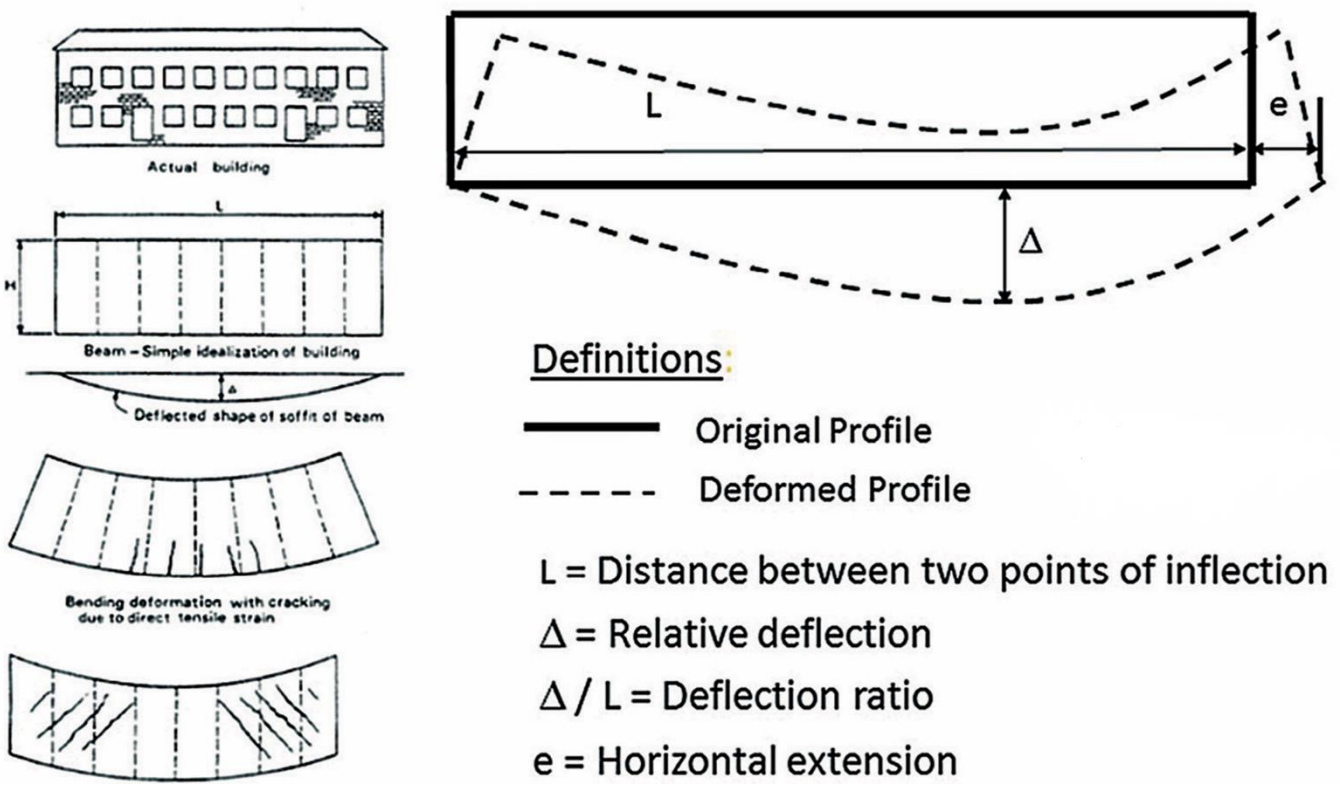

Figure 11. Elastic beam model for buildings.

The evaluation consists of three phases summarized in the next page:

Phase 1: In the first phase, buildings were classified as Damage Category 1 ('very slight') Table 10 if they had minor issues, like predicted ground movement from bored tunnels or excavations of less than 10mm and a ground slope of less than 1/500, based on Rankin's earlier definitions [43], and these buildings did not need any more evaluation. This phase comprised an initial screening using upper-bound parameters and assumed greenfield conditions.

Table 10. Building damage classification

Risk category	Max tensile strain (%)	Description of degree of damage	Description of typical damage and likely form of repair for typical masonry buildings	Approx. crack width† (mm)
0	0.05 or less	Negligible	Hairline cracks	
1	>0.05 and ≤0.075	Very slight	Fine cracks easily treated during normal redecorations. Perhaps isolated slight fracture in building. Cracks in exterior brickwork visible upon close inspection	0.1 to 1
2	>0.075 and ≤0.15	Slight	Cracks easily filled. Redecoration probably required. Several slight fractures inside building. Exterior cracks visible; some repointing may be required for weathertightness. Doors and windows may stick slightly	1 to 5
3	>0.15 and ≤0.3	Moderate	Cracks may require cutting out and patching. Recurrent cracks can be masked by suitable linings. Repointing and possibly replacement of a small amount of exterior brickwork may be required. Doors and windows sticking. Utility services may be interrupted. Weathertightness often impaired	5 to 15 or a number of cracks greater than 3
4	>0.3	Severe	Extensive repair involving removal and replacement of sections of walls, especially over doors and windows required. Windows and door frames distorted. Floor slopes noticeably. Walls lean or bulge noticeably, some loss of bearing in beams. Utility services disrupted	15 to 25 but also depends on number of cracks
5		Very severe	Major repair required involving partial or complete reconstruction. Beams lose bearing, walls lean badly and require shoring. Windows broken by distortion. Danger of instability	Usually greater than 25 but depends on number of cracks

Phase 2: In the next phase, a generic assessment was performed for buildings within the 10mm settlement contour. The greenfield settlement was imposed on buildings, assuming that the settlement behavior is not modified by the stiffness of the building, which is taken to be completely flexible. Additionally, the deformation resulted from horizontal ground movement was deemed. As it is demonstrated in Fig. 11, the simplified elastic beam model for the simple case where a building is located transverse to a tunnel below and entirely within the sagging zone of the settlement trough. Also, a building's response to the settlement

is impacted by the relative location of the building in relation to the sagging or hogging profile of the settlement trough. Using the procedure described by Burland [40], the risk category for each building was assessed as defined in Table 10.

Phase 3: In the last phase, buildings were taken into account individually rather than as part of an area analyzed generically. In phase 3 assessment, several iterations were used as needed, the intention being to understand whether increasing levels of accuracy would credibly reduce the risk of damage to an 'acceptable' level. Numerical modeling of the soil structure interaction associated with the tunnel excavation and a more detailed assessment of the actual structure were done. Moreover, visual inspections were undertaken by structural engineers related to heritage for the listed buildings in order to take into consideration their form and condition. The sensitivity assessment of listed structures was scored and illustrated in Table 11.

Table 11. Scoring for sensitivity assessment of listed buildings

	Criteria	
Score	**Sensitivity of structure to ground movements and interaction with adjacent buildings**	**Sensitivity to movement of particular features within building**
0	Masonry building with lime mortar not surrounded by other buildings. Uniform facades with no particular large openings	No particular sensitive features
1	Buildings of delicate structural form or buildings sandwiched between modern framed buildings which are much stiffer, perhaps with one or more significant openings	Brittle finishes, e.g. faience or tight-jointed stonework, which are susceptible to small movements and difficult to repair
2	Buildings which, by their structural form, will tend to concentrate all their movements in one location	Finishes which, if damaged, will have significant effect on heritage of building, e.g. cracks through frescos

4.4.4 Approaches to mitigation

4.4.4.1 General approaches

For the number of properties within the zone of influence of the project with regard to the range of construction types, age, and use, it was reasonable to anticipate some degree of pre-existing deterioration in at least some of these buildings. Defect surveys were carried out in advance of the works to provide a record of the pre-works condition as a reference for agreeing to any changes that could be assigned subsequently to the works. Around the stations, where demolition of adjacent buildings was required, the influence of these preliminary works was assessed, and defect surveys were undertaken prior to the beginning [44].

4.4.4.2 Ground Treatment

In the places, such as around stations and shafts, where the estimation of collapse is high, compensation grouting was adopted as the principal means of mitigation. While this did not control settlements to an absolute target value, it reduced the unmitigated movement and, more importantly, was used to limit the deflection ratio (Fig. 11) to a value consistent with damage category 1, very slight or less (Table 10).

Compensation Grouting: A grout shaft is installed at a specified location to enable an array of tubes à manchette (TAMs) to be drilled out horizontally to lengths of up to 80m from the shaft. The tubes are installed radially at a number of depths within the shaft (Fig. 12). Grout is injected through a selected TAM using two rubber packers, which select the part of the tube where the grout will be injected. The grout is injected at high pressure so that the ground is fractured horizontally. Then, the grout penetrates through the fractured cracks and heaves the ground to compensate for settlements (Fig. 13). The installation of the grout shaft and TAMs themselves causes some ground settlement, even though compensation grouting is intended to mitigate ground movement. While vertical ground movements due to the installation of the shaft are insignificant, the TAM installation process can cause settlement, in some cases of a magnitude of 10–20mm, influenced by ground conditions, and this initial settlement is later compensated for by injecting grout through the TAMs before the main tunnel construction work starts.

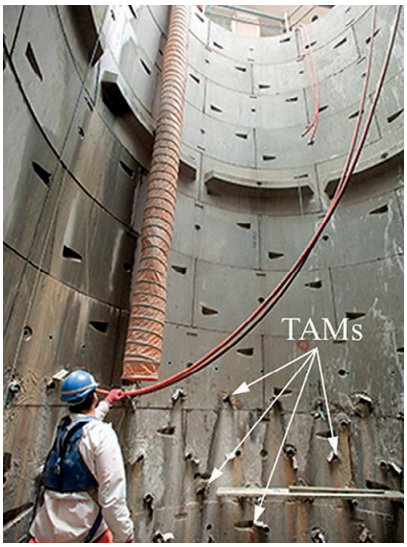

Figure 12. Compensation grouting shaft with TAM array installed.

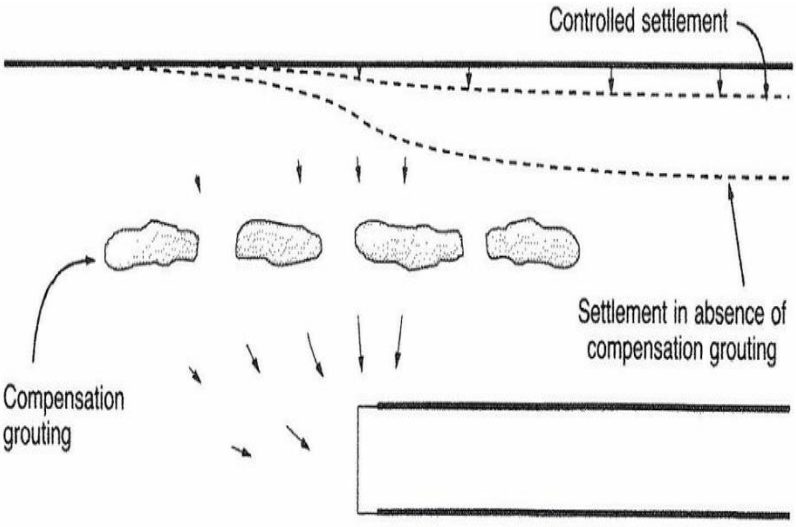

Figure 13. Principals of compensation grouting.

4.4.4.3 Monitoring

One of the most important parts of the asset protection strategy is monitoring both buildings and the ground, which was undertaken extensively across the project. This provided information on when and how contingency measures should be adopted. It confirmed that the ground and the assets were behaving as anticipated. It also both provided information for design verification and allowed construction control, providing confirmation that excavations were being implemented in a controlled manner. Some techniques, including manual monitoring and leveling by using invar calibrated scales (Fig. 14a); automated monitoring by using automated monitoring total stations done by prisms on building facades (Fig. 14b); and controlling building slopes by using hydrostatic leveling cells (Fig. 14c), were used to check and supervise the situation.

Figure 14a. Invar on building facade.

Figure 14b. Prism on building facade.

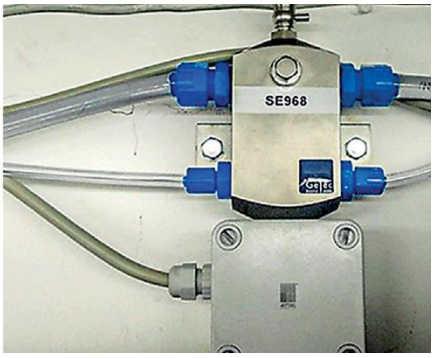

Figure 14c. Hydraulic leveling cell.

At a later stage, satellite technology was used to look at ground movements in specific areas. This is an area where there are continuing developments, and some changes might be anticipated for subsequent projects [44].

5. Hydraulic Project
5.1 Introduction

This project is the real-world case that is related to the construction tunnel of a sewerage system designed to guarantee the future reliability of sewerage network. It aims to enhance the capacity, reliability, and environmental sustainability of the sewerage network. The total tunnel length is 14.3 km, and the project is located in the urban area with high population density.

5.2 Analysis methodology for buildings

The excavation of tunnels in urban areas necessarily causes a disturbance in the ground, inducing subsidence in the buildings and structures falling within the area of influence of the excavation (ZOI). For this reason, the construction of underground structures in urban areas requires an analysis of the problems related to excavations. As stated in the previous parts, the risk analysis for pre-existing buildings is based on the following two essential elements, also known as BCS (Building Condition Survey) and BRA (Building Risk Assessment). The procedure used to determine the effects induced by excavations on surrounding buildings has been described before (Fig. 4). The analysis was conducted in two phases that developed simultaneously. On the one hand, the current state of consistency of the buildings was verified, therefore representative of the susceptibility of the buildings to suffer damage caused by movements in the foundation soil. On the other hand, the deformation state induced by the excavation of the tunnel and the stations in the ground was evaluated, assuming that the building subjects deformations equal to those of the soil. Some control parameters were monitored and compared with conventional thresholds representing different levels of damage. The thresholds were modified according to the initial degree of conservation of the building. The calculation method adopted is based on empirical relationships, widely confirmed by previous experiences and by the reference scientific literature [2], [31], [45], and allows us to evaluate the size and shape of the subsidence basin deriving from the excavation.

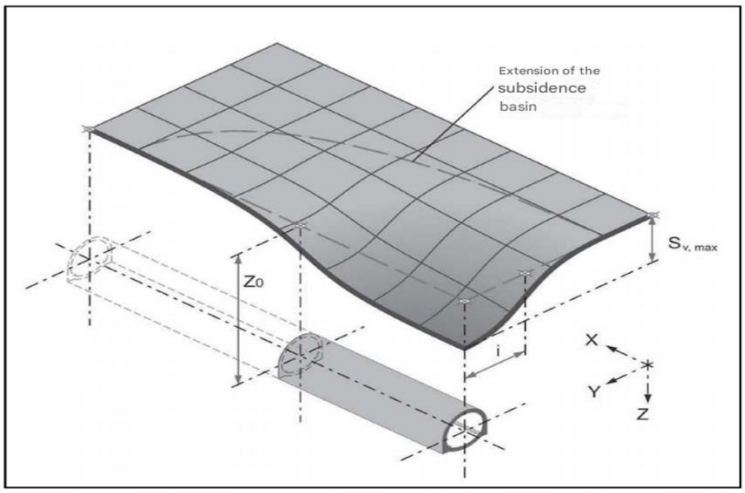

Figure 16. Subsidence basin induced by the advance of tunnel excavation

The vertical displacements S_v of the ground level points arranged along a generic cross section orthogonal to the tunnel axis, are calculated through the following empirical expression:

$$S_v = S_{max} \exp\left(\frac{-Y^2}{2\,i^2}\right)$$

Where:

- S_{max} is the maximum settlement at the vertical axis of the tunnel.
- Y is the horizontal distance from the tunnel axis of the generic point on the ground level.
- i is the horizontal distance from the tunnel axis of the inflection point of the settlement curve.

For the parameter i, it is assumed that it varies linearly with the depth Z_0 of the tunnel axis, so:

$$i = k \,.\, Z_0$$

This expression was suggested by O'Reilly and the value used for the constant k depends on the characteristics of the soils involved and the depth of the excavation. As a guide, values can be assumed ranging from 0.20 to 0.40 in sands, 0.40 and 0.60 in consistent clayey soils, and 0.60 and 0.75 in soft clayey soils. The analytical structure is the Gaussian distribution curve and its typical trend is represented below.

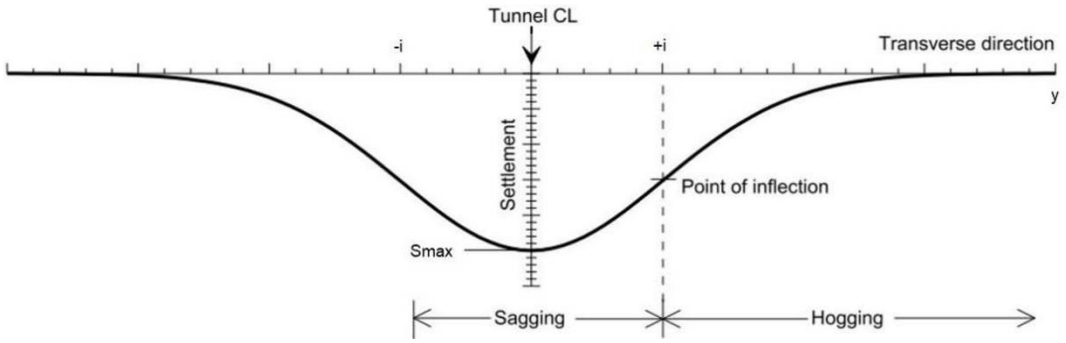

Figure 17. Trend of vertical displacements for a cross-section of the tunnel

If the subsidence trend is well represented by the Gaussian curve, the volume of the subsidence basin V_s is equal to:

$$Vs = i\sqrt{2\pi}\, S_{max}$$

From which the maximum settlement value can be obtained:

$$S_{max} = \frac{V_s}{i\sqrt{2\pi}}$$

The method is also based on the evaluation of the percentage volume loss V_p induced by the excavation, defined as the ratio between the volume of the subsidence basin and the theoretical excavation volume of the tunnel, measured over a unit distance. The values of the volume loss are generally chosen on the basis of experience for each type of excavation method and for each ground condition. In cases where excavation machines with a back-pressure face of the ground have been used, the typical design values are in the order of 0.5-1.0 percent. The correlation between V_p and V_s is reported in the following formula:

$$Vs = A \,.\, Vp$$

Therefore, the value of the maximum settlement in the tunnel axis can be expressed as a function of the tunnel diameter, the abscissa of the inflection point of the settlement curve i, and the volume loss V_p:

$$S_{max} = \frac{\pi}{4\sqrt{2\,\pi}} \frac{V_p\, D^2}{i}$$

Starting from the equation of the vertical displacements, it is possible to obtain the trend of the rotations and curvatures by derivation. The expressions relating to the rotation θ (first derivative of the displacement) and curvature χ (second derivative of the displacement) are given below:

$$\theta = \frac{S_{max}}{i^2} \exp\left(\frac{-Y^2}{2\,i^2}\right)$$

$$\chi = \frac{S_{max}}{i^2} \cdot \left[\frac{Y^2}{i^2} - 1\right] . \exp\left(\frac{-Y^2}{2\,i^2}\right)$$

The determination of the tensile deformation in buildings requires knowledge of the horizontal movements S_h of the ground level, so some tools necessary for their calculation are provided below. Assuming that the displacement vector of a generic point on the ground surface located on the abscissa y has a direction defined by the line joining the point itself with the center of the tunnel, simple geometric considerations allow us to write:

$$S_h = \frac{y}{Z_0} \,.\, S_v$$

From which by derivation it is possible to obtain the consequent deformation of the ground. The expression of the horizontal deformation ε_h is given below (derivative before the horizontal displacement):

$$\varepsilon_h = \frac{S_v}{Z_0} \cdot \left[1 - \frac{Y^2}{i^2}\right] \cdot \exp\left(\frac{-Y^2}{2\,i^2}\right)$$

Figure. 18 shows the typical trend of S_h compared with the curves that define the vertical displacements S_v and the ground deformations ε_h. The figure also highlights the strip of ground between the two inflection points of the settlement curve within which the deformations are compressive (negative ε_h). The identification of these points will therefore be of crucial importance when the resulting deformations in buildings must be determined, since outside this region these deformations will be added to the tensile ones that arise from the settlements, with a consequent worsening in the stress-strain regime of the structure.

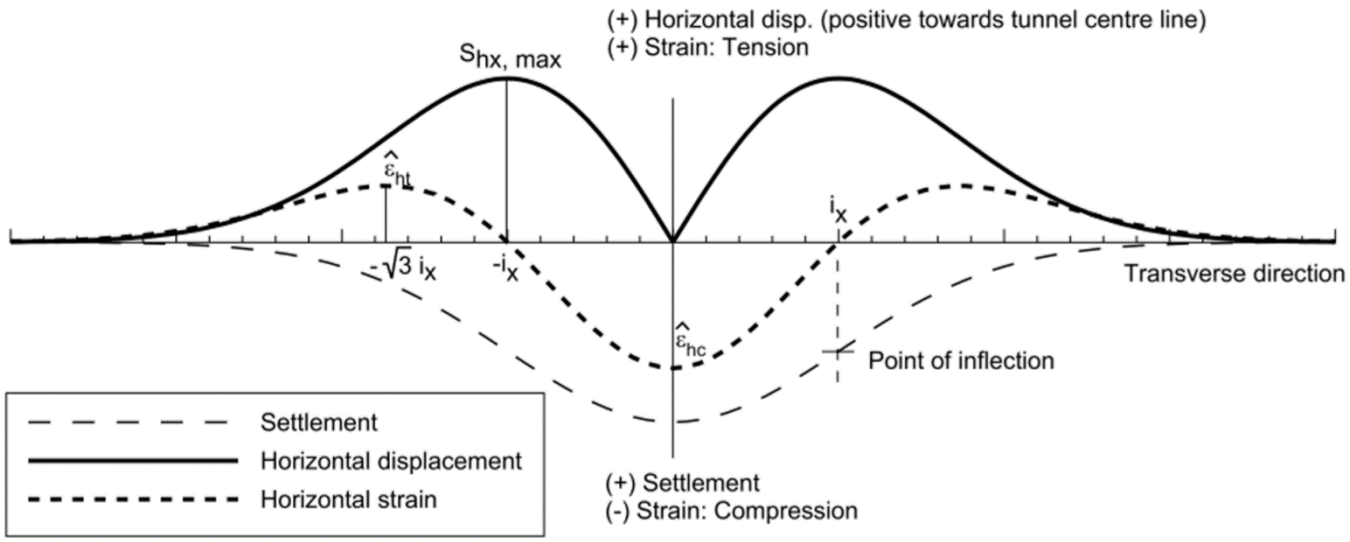

Figure 18. Qualitative distribution of vertical and horizontal settlements and horizontal deformations.

In the figure above, it is clear how the settlement curve can be divided into three distinct zones:
Two with downward concavities (hogging zones) included in the intervals:

$y \leq -i_x$ and $y \geq i_x$

An upwardly concave area (sagging zone) within the range.

$$-i_x \leq y \leq i_x$$

The above considerations are valid for settlements induced on the surface. However, if one wants to know the settlement at the foundation plane by replacing (z_0-z), with z depth of the foundation plane, one risks overestimating the maximum settlement and underestimating the width of the subsidence curve (S_{max} greater and i less).

If monitoring results are available for calibration, it is possible to refine the solution using the formulation of Moh [46], in which the parameter m to be calibrated appears. In the case in question m=1 and b=k have always been considered.

$$i_z = bD\left(\frac{z_0 - z}{D}\right)^m = i_0\left(\frac{z_0 - z}{z_0}\right)^m$$

5.3 Effects on buildings

To define more precisely the behavior of buildings with respect to subsidence and, therefore, to identify the parameters that most induce damage to the structures, it is necessary to make an initial distinction based on the type of foundations:

• Continuous foundations: this category includes all buildings founded on a foundation slab, on stone plinths, on wooden piles and, in some cases, on reinforced concrete piles;

• Isolated foundations: this category includes all buildings founded on reinforced concrete plinths, and, in some cases, on reinforced concrete piles.

It is therefore necessary to first identify the identifying parameters of the induced deformation state as a function of the structural typology and the foundations, and to associate these with "risk categories" delimited by characteristic values. In summary, these identifying parameters can be identified according to the following points:

• For structures characterized by continuous foundations, the damage assessment parameter is given by the maximum tensile deformation undergone by the building (ε_{max}), which is a function of the maximum relative deflection (Δ_{max}) undergone by the building. The maximum tensile strain must be compared with the limit tensile strain (ε_{lim}) given by the classifications.

• For structures on isolated foundations the damage is mainly caused by the differential settlement between the plinths. The most important parameters, in this case, are the maximum angular distortion β_{max} and the maximum settlement S_{max} suffered by the building (see Fig. 5). With regard to the extent of the damage, the induced damage can be classified into Aesthetic, Functional, and Structural damage explained in chapter 4.3.

For structures with a foundation typology defined as continuous, the reference values for the parameter for evaluating possible damage (the tensile limit strain) are provided by the Burland classification (Table 6), which identifies different risk categories, based on the cracking state of the structure. For buildings with isolated foundations, it is the Rankine classification (Table 7) for the identification of the different risk categories.

Vulnerability is defined as an intrinsic characteristic of the building (dependent on its history but independent of external factors that can induce differential subsidence at the level of its foundations), which expresses how much the building deviates from the conditions of perfect conservation and, therefore, how vulnerable it is. The greater the vulnerability of the building, the lower its ability to tolerate further deformations induced by external events. Vulnerability is expressed through an index, which is

called vulnerability index Iv (Table 4). The vulnerability index is used to establish a reduction factor of the limit values of the control parameters that appear in the risk classifications, which are generally referred to buildings in a good state of conservation, precisely to take into account the particularity of the history of each building that, over time, can reduce its response capacity.

The Table 12 highlights the subset of Damage Categories / Vulnerability Classes of the buildings resulting from the analyses and checks carried out in this design phase. All the buildings fall into damage categories lower than the second, with the exception of a non-significant exception (disused building not habitable), in the various risk scenarios, as better described in the following chapters.

Table 12. Correction of the value ranges for the control parameter in potential damage classification based on Iv

Damage Category	Control Parameters	Irrelevant (0<Iv<2) Fr=1.0	Low (2<Iv<4) Fr=1.25	Medium (4<Iv<6) Fr=1.5	High (6<Iv<8) Fr=1.75	Very High (8<Iv<10) Fr=2.0
1	S_{max} [mm]	<10	<8	<6.7	<5.7	<5
	β_{lim} [%]	1/500	1/625	1/750	1/875	1/1000
	S_{lim} [%]	min 0.000 max 0.075	min 0.000 max 0.060	min 0.000 max 0.050	min 0.000 max 0.043	min 0.000 max 0.038
2	S_{max} [mm]	10–50	8–40	6.7–33.3	5.7–28.6	5–25
	β_{lim} [%]	1/200	1/250	1/300	1/350	1/400
	S_{lim} [%]	min 0.075 max 0.150	min 0.060 max 0.120	min 0.050 max 0.100	min 0.043 max 0.088	min 0.038 max 0.075
3	S_{max} [mm]	50–75	40–60	33.3–50	28.6–42.9	25–37.5
	β_{lim} [%]	1/50	1/62.5	1/75	1/87.5	1/100
	S_{lim} [%]	min 0.150 max 0.300	min 0.120 max 0.240	min 0.100 max 0.200	min 0.086 max 0.171	min 0.075 max 0.150
4	S_{max} [mm]	>75	>60	>50	>42.9	>37.5
	β_{lim} [%]	1/50	1/62.5	1/75	1/87.5	1/100
	S_{lim} [%]	min >0.300	min >0.240	min >0.200	min >0.171	min >0.150

In addition to the classification criterion mentioned above, the indications were accepted in terms of maximum subsidence and inclinations (threshold values for monitoring and control during the excavation

progress) indicated below Table 13. In fact, an initial identification of the buildings to be paid attention to within the set of buildings surveyed was carried out considering the threshold values.

Table 13. Monitoring threshold values for buildings and roads

DATA	MAXIMUM SETTLEMENT	MAXIMUM INCLINATION
Buildings in R.C. and low-level masonry (2 floors above ground) and garages	10 mm	1/500
High masonry buildings (more than two floors above ground) or historic buildings	10 mm	1/1000
Roads or parking areas	10 mm	1/250
Parks	40 mm	1/250
Reaching **threshold values** (warning values)	The contractor must provide additional methods and change operational procedures to limit displacement	
Reaching **limit values**	The contractor must immediately stop all work and present an action plan before resuming work	

The criteria previously described for the evaluation of the Damage Classes are valid in the context of the impact studies of the buildings. For the other interferences present in the route, specific analyses were carried out on the dimensional characteristics of the interferences with respect to the subsidence curves defined along the route of the work shown below.

Table 14. Threshold values for monitoring sewer structures, underground canals, tunnels, and large aqueducts

Threshold values for tunnel excavation displacement	Limit values requiring work stoppage
Horizontal or vertical displacement **5 mm**	Horizontal or vertical displacement **10 mm**
If the threshold is reached, the contractor must provide additional means and methods to change operational procedures to limit displacement.	If the limit is reached, the contractor must stop all work immediately and present an action plan before resuming.

5.4 Subsidence analysis and risk categories
5.4.1 Sensitivity analysis on the influence of key parameters and coverage

In order to define the reference parameters for the subsidence assessment, a sensitivity analysis was performed on the basic parameters, such as the depth of the tunnel axis from the ground level Z_0, the percentage of volume loss V_p and the parameter k. Knowing that the depth of the axis, for the sensitivity analysis with respect to the parameter Z_0, a variation range was chosen between 14m and 30m with a step of 2m, setting the remaining parameters: k=0.3 and V_p=1%. In the Figure. 19 below, it is clear how the variability of the depth of the tunnel axis from the ground level influences the extension of the basin of the subsidence curve and the value of its maximum settlement. For smaller coverages it is possible to expect a narrower basin with a greater maximum settlement value that exceeds 9 mm for depths Z_0 close to 14 m, where however there are no buildings or other significant infrastructures.

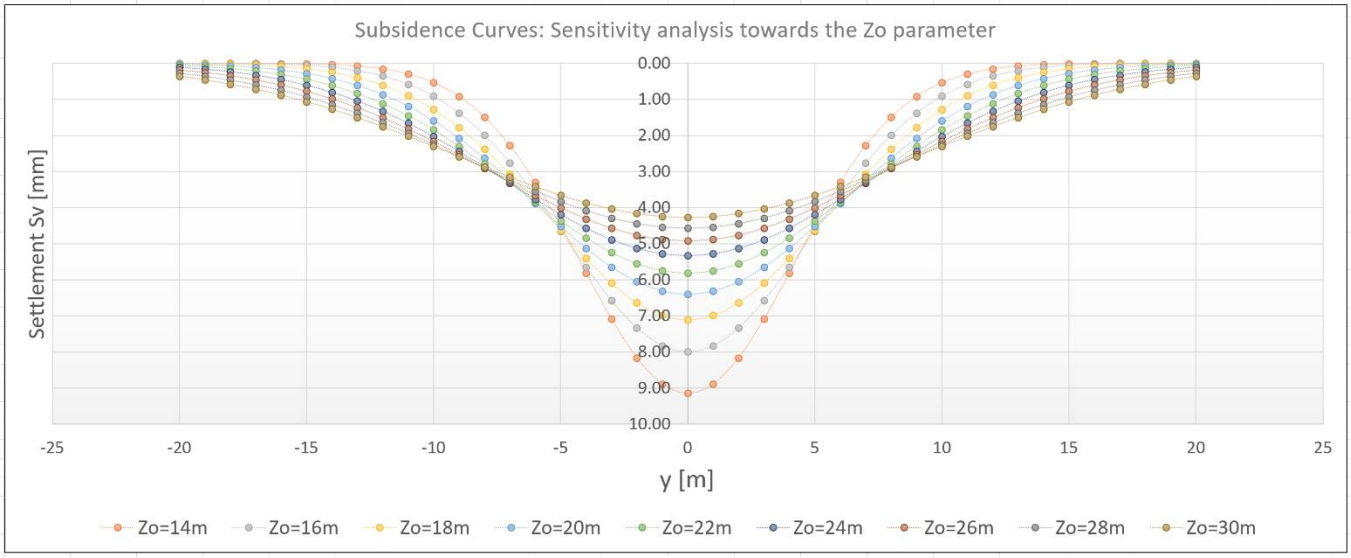

Figure 19. Subsidence curves: sensitivity analysis towards the Zo parameter (k=0.3 Vp=1%)

As regards the V_P parameter, 0.5% and 2% were chosen as the extreme values of variability. The sensitivity analysis was conducted with a value of k=0.3 and Z_0=23m (minimum coverage conditions in the presence of works in the potential influence zone), highlighting that the increase in the volume percentage extends the area under the curve and consequently the maximum subsidence (see Fig. 20). The reference scenario foresees a loss of volume equal to 1% which in the conditions of average depth of the axis of the tunnel

(Z_0=23m), determines a maximum settlement greater than 5mm. A volume loss of 2% in the same depth conditions exceeds the 11mm maximum settlement.

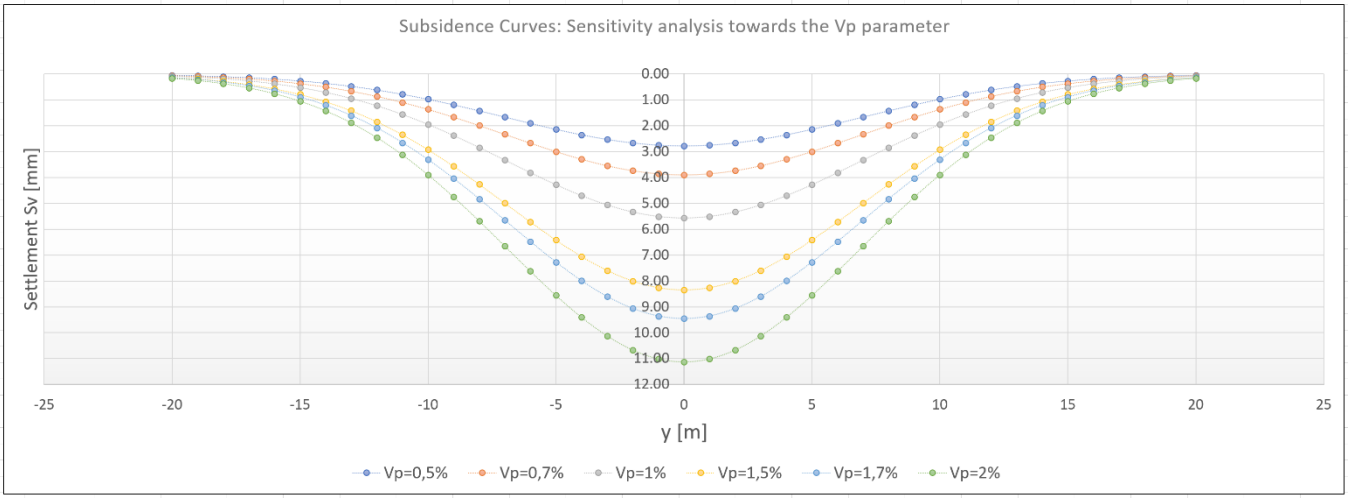

Figure 20. Subsidence curves: sensitivity analysis towards the Vp parameter (k=0.3 Z_0 =23m)

Finally, the sensitivity analysis was performed with respect to the parameter k, setting V_P =1% and Z_0=23m and a variability of k between 0.3 and 0.5. The increase of the parameter k reduces the maximum settlement and moves the inflection points away from the vertical axis passing through the center of the tunnel (see Fig. 21). As can be seen from the graph in the figure, the increase of the parameter k reduces the maximum settlement, but increases the distortion.

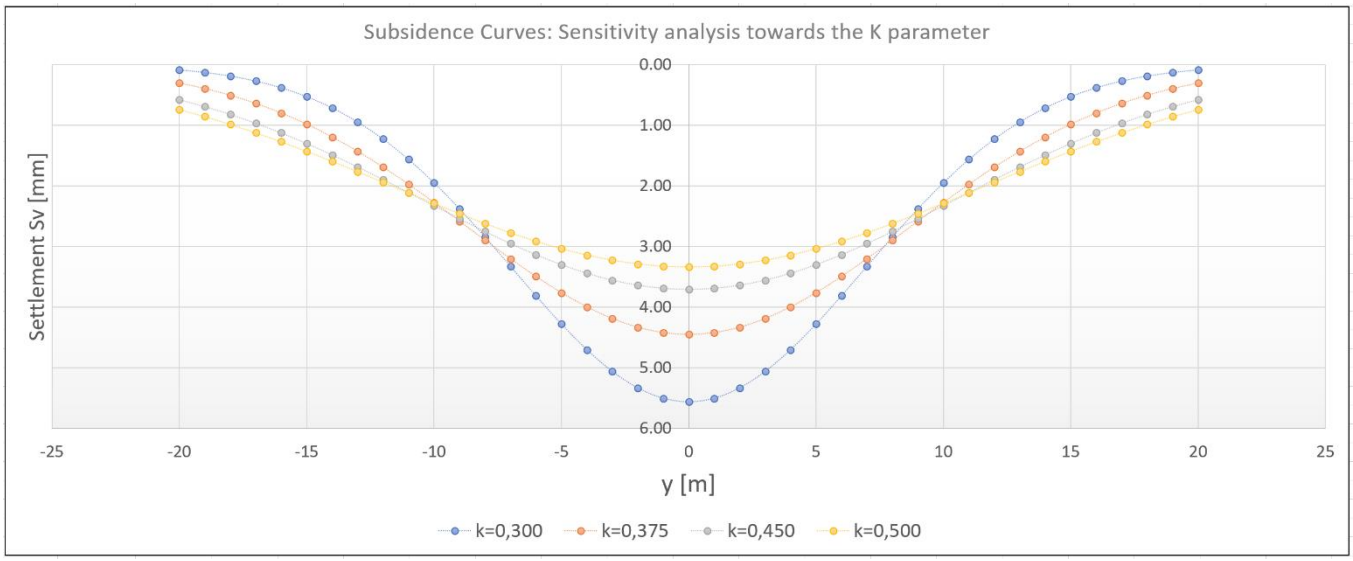

Figure 21. Subsidence curves: sensitivity analysis towards the Vp parameter (Vp=1% Z_0 =23m)

5.4.2 Selection of key parameters and results of subsidence analyses

Based on the results of the sensitivity analyses and the experiences following project scenarios for subsidence analyses have been defined:

Table 15. Project scenarios

Project Scenarios	K [-]	V_P [%]
Reference scenario	0.3	0.5
Pessimistic baseline scenario	0.3	1
Emergency scenario	0.3	2

In particular, the choice of the value of k for the various scenarios is based on the results obtained during the design and construction of the other project placed near the location of the project. Therefore, it was possible to establish that a value of k equal to 0.3 is well representative of the urban soil. As regards the choice of the Lost Volume, which depends, as is known, on both the geomechanical characteristics of the ground and on the excavation method and machine, it was deemed reasonable to consider for the reference scenario a percentage loss of volume equal to 0.5%, since the planned excavation will be carried out using a Slurry TBM, capable of obtaining greater control of the pressures at the face. The calculation of the subsidence curves and relative iso-subsidence curves was carried out along the route calculating a Gaussian curve every 5 m and graphically interpolating the results shown below (Fig. 22, 23, 24):

Figure 22. Settlement curves (K= 0.3, Vp = 0.5%)

Figure 23. Settlement curves (K= 0.3, Vp = 1%)

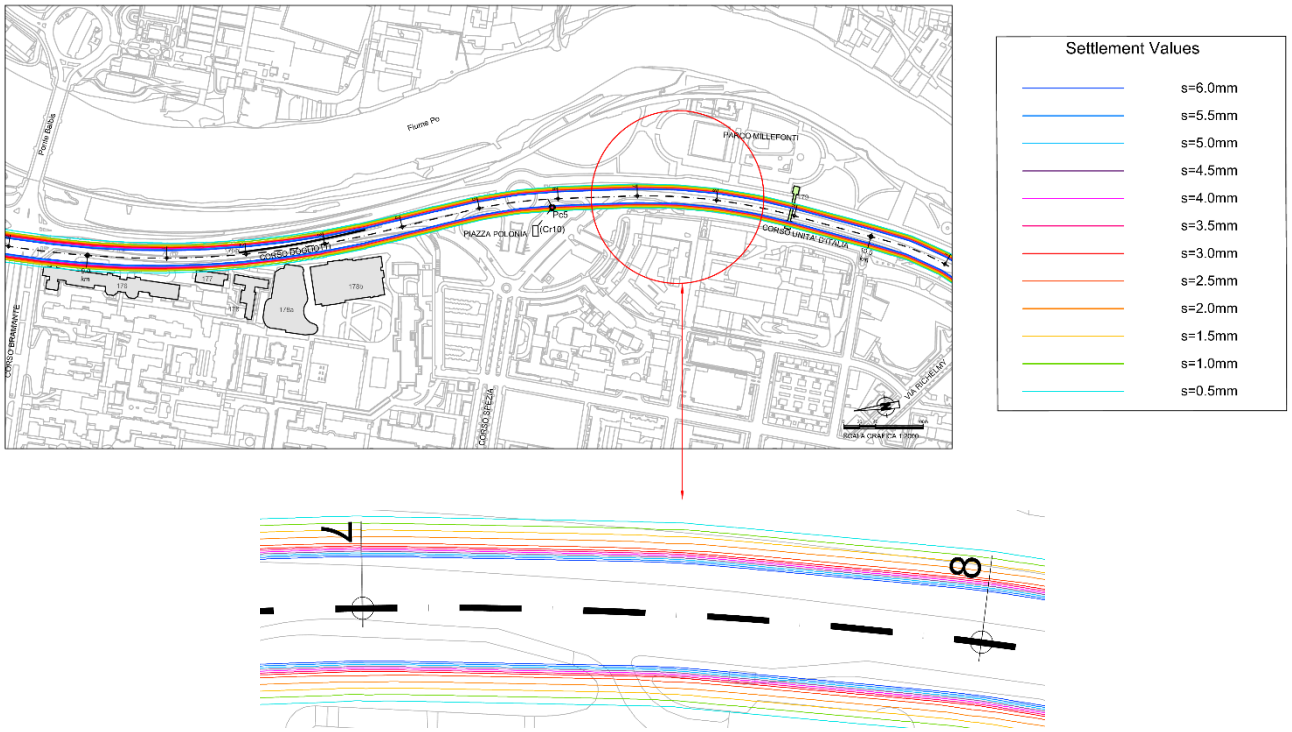

Figure 24. Settlement curves (K= 0.3, Vp = 2%)

5.4.3 Damage category for buildings

The calculation of the control parameters defined previously, which is useful for determining the damage class of the buildings, was carried out for some buildings. For each building, the subsidence curve was then represented, belonging to the pessimistic reference scenario with k=0.3 and V_P=1%. Below, some examples are shown below:

Table 16. Building Features

Building Code: 104	
K [-]	0.3
Vp [%]	1%
Control Parameters	
β	1/7143
S_{max} [mm]	4.29
ε_r [%]	0.021
Vulnerability Index	
Medium	4.75

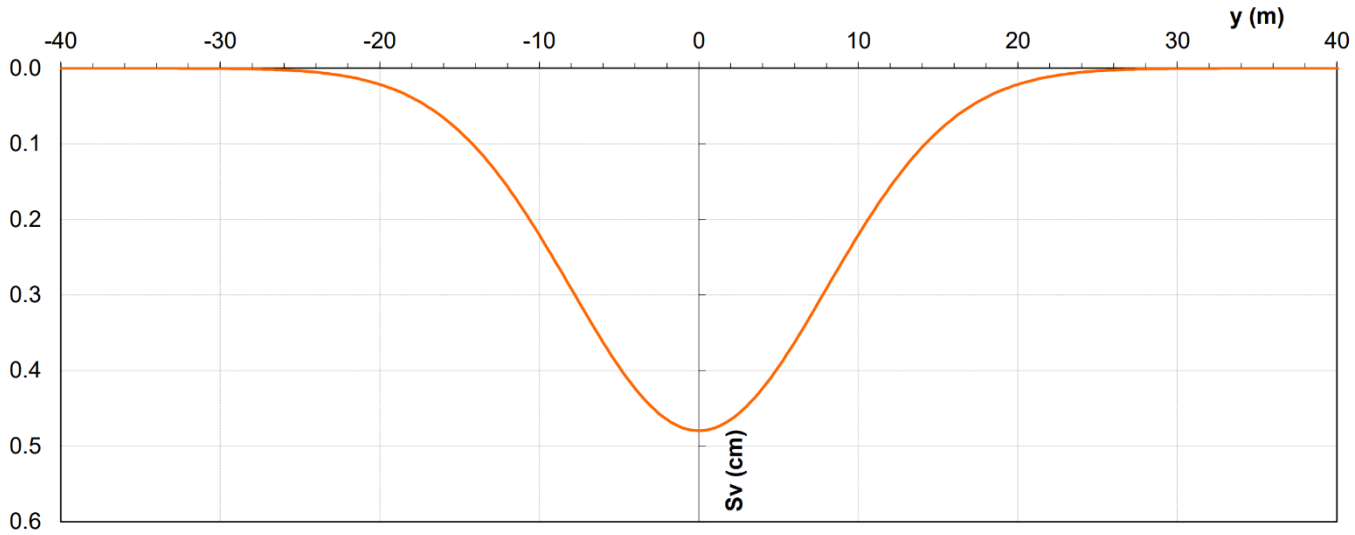

Figure 25. Vertical Settlement

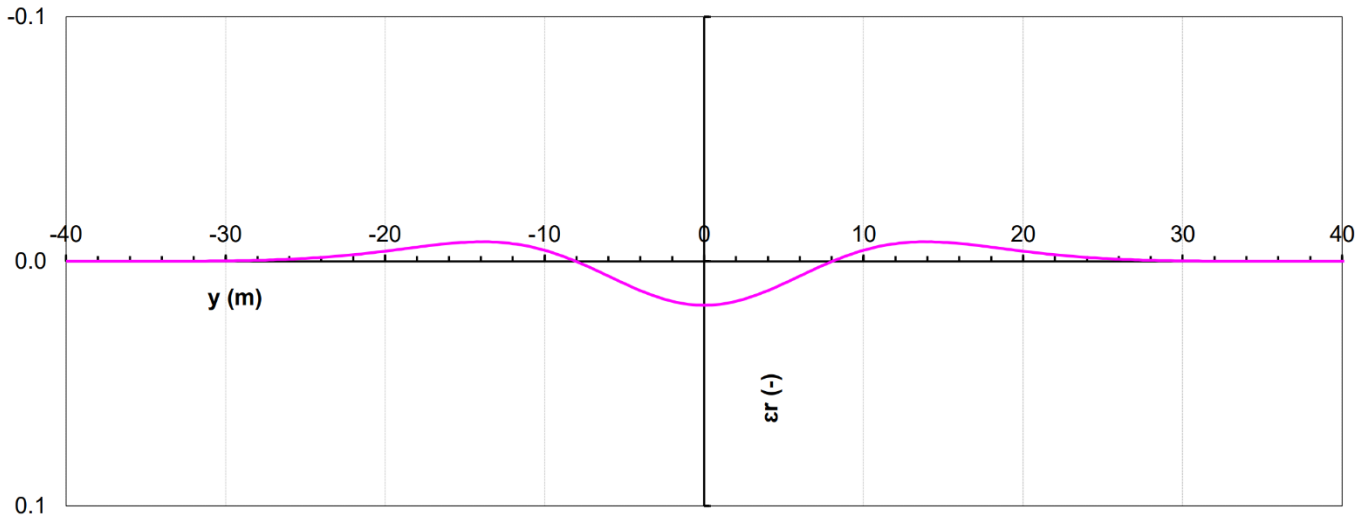

Figure 26. Horizontal Deformation

Table 17. Building Features

Building Code: 73	
K [-]	0.3
Vp [%]	1%
Control Parameters	
β	1/9992
S_{max} [mm]	3.79
ε_r [%]	0.014
Vulnerability Index	
Low	3.69

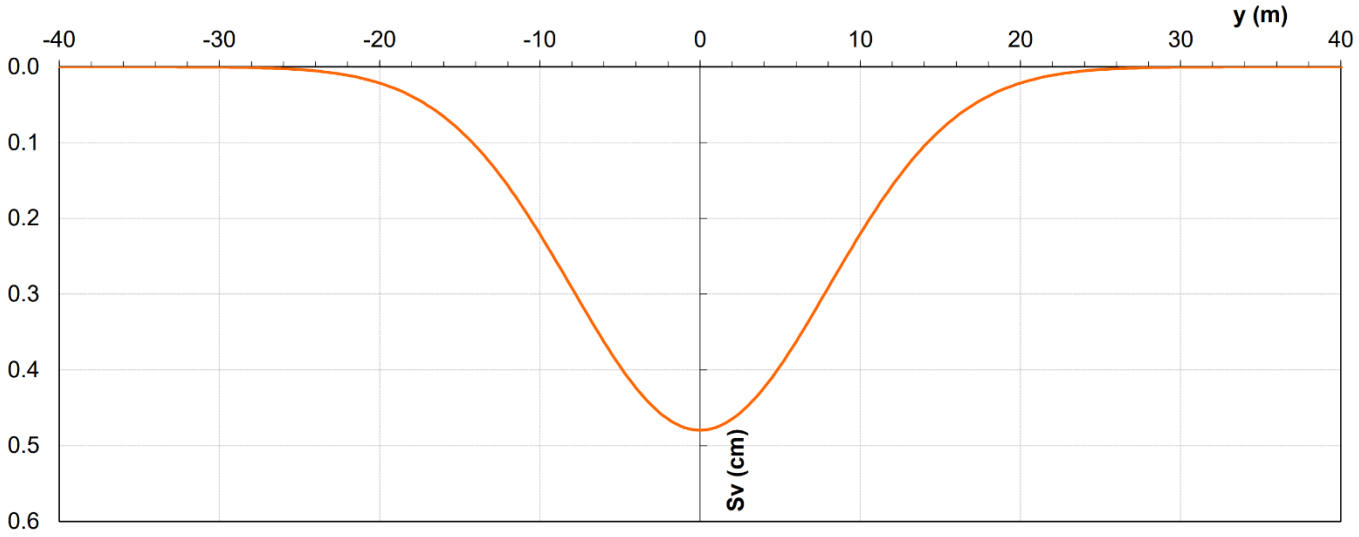

Figure 27. Vertical Settlement

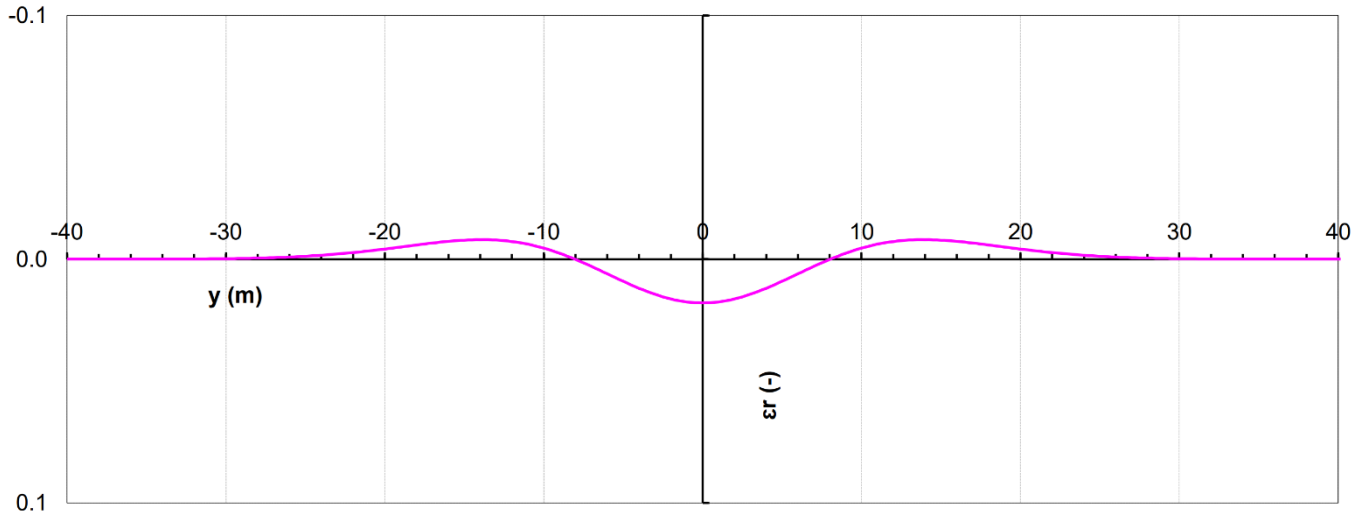

Figure 28. Horizontal Deformation

5.4.4 Mitigation measures and countermeasures

During the construction phase and during the works, it is essential to define a flexible strategy to manage the residual risk (countermeasures). This strategy mainly includes the adoption of the Monitoring and Control (M&C) measures described briefly below:

• Implementation of the Tunnel Advancement Protocol: Based on the knowledge acquired in the previous sections, the detailed construction project is developed by the sections, which can improve the quality of the knowledge used in progress.

• The implementation of an automated, centralized monitoring system will provide real-time access to information and all georeferenced results through the GIS (Geographic Information System), which is applied to monitor underground excavation. This integrated data management system is designed as a communication tool for the project participants and aims to facilitate knowledge capitalization, making it accessible via the Internet.

• Real-time management through GIS to monitor information and machine data related to the results of geognostic surveys, studies, and investigations on buildings, environmental studies, and construction data continuously comparable with the project hypotheses and with the levels of control (attention and alarm) defined along the route and for specific works.

The criterion for determining which interventions to carry out was based on the improvement of the mechanical properties of the medium (ground) between the work in progress (tunnel) and the one (building) to be protected. Two possible intervention schemes were identified:

• Sub-vertical partition: the ground between the tunnel and the building can be consolidated with injections through valved pipes laid in vertical or inclined holes. This intervention scheme can be implemented when the distance between the tunnel and the building to be protected is greater than a few meters and it is therefore possible to obtain a band of consolidated soil with adequate thickness created with conventional methodology and equipment. The purpose of the sub-vertical partition is to create a barrier to potential

subsidence induced by the excavation of the tunnel, preventing their propagation to the foundation level of the building.

• Sub-horizontal partition with compensation grouting: the ground between the tunnel and the building can be consolidated with injections through valved pipes laid in sub-horizontal holes. This intervention scheme must be implemented when the interferences and reciprocal geometric positions of the tunnel and the building to be protected do not allow the execution of sub-vertical and/or inclined partitions that can be achieved with conventional equipment.

The treatment with compensation grouting consists in the consolidation of the material under the foundations of the building, through horizontal (or sub-horizontal) perforations performed from the surface or from a well. The intervention allows, by injecting in a controlled manner cement mixtures under pressure, to "compensate" the settlements found with corresponding rises induced by means of the injections. The “jack” effect is exploited by the compensation injections, the location and amount of which is decided on the basis of the monitoring readings available in real time.

6. Conclusions

This thesis has investigated various aspects related to tunneling-induced settlements in urban environments by a detailed review of soil behavior, settlement mechanisms, prediction models, and practical mitigation strategies. The relationship between geotechnical conditions and tunneling methods is essential for minimizing surface deformations. For example, cohesive soils experience significant long-term settlements due to primary consolidation and creep, while in cohesionless soils, erosion and progressive instabilities are crucial factors.

Both empirical and analytical models are still effective tools to estimate settlement profiles. Empirical models offer a simple way to estimate settlement, but they are constrained to specific ground conditions. Analytical approaches provide better accuracy by considering soil-structure interactions but require precise parameter calibration.

The Building Condition Survey (BCS) and Building Risk Assessment (BRA) quantify building vulnerability through defect mapping and vulnerability index (I_V) scoring. Damage thresholds (e.g., Burland's tensile strain limits, Rankin's angular distortion) must be adjusted for pre-existing conditions, and for high-risk structures, more attention and controls are needed. Urban tunneling projects must prioritize early BCS, real-time data integration, and adaptive construction (e.g., TBMs, NATM) to minimize risks.

The sensitivity analysis in case studies validates that the percentage of volume loss (Vp), the depth of the tunnel axis from the ground level (Z0), and parameter (K) are influential factors related to settlement. Compensation grouting, real-time monitoring and control through GIS, and automated monitoring (e.g., hydrostatic cells, satellite technology) are critical for controlling settlements and phased BRA to protect the structures that are affected by tunneling excavation.

Finally, this study emphasizes the importance of combining geotechnical knowledge with risk management in urban tunneling projects. It concludes that by combining theoretical aspects with real-world cases, there is safer and more reliable underground infrastructure development in the urban areas.

References

[1] Mair, R. J., & Taylor, R. N. (1997). "Bored tunneling in the urban environment." Proceedings of the 14th International Conference on Soil Mechanics and Foundation Engineering.

[2] Peck, R. B. (1969). "Deep excavations and tunneling in soft ground." State-of-the-Art Report, 7th International Conference on Soil Mechanics and Foundation Engineering.

[3] Verruijt, A., & Booker, J. R. (1996). "Surface settlements due to deformation of a tunnel in an elastic half-plane." Géotechnique.

[4] Burland, J. B. (2001). "Assessment of risk of damage to buildings due to tunneling and excavation." Proceedings of the Institution of Civil Engineers - Geotechnical Engineering.

[5] Gens, A., Arroyo, M., & Alonso, E. E. (2006). Ground response to tunnel construction: Barcelona case study. *Géotechnique*.

[6] Schubert, W. (1996). Experiences with NATM in Urban Areas: Munich Metro Project. *Tunneling and Underground Space Technology.*

[7] Mechanized Tunneling in Urban Areas: design methodology and construction control / edited by Vittorio Guglielmetti, Ashraf Mahtab & Shulin Xu (2008).

[8] Mair, R. & Taylor, R. (1997). Theme lecture: bored tunneling in the urban environment. Proceedings of XIV ICSMFE, 1999. London, UK: International Society for Soil Mechanics and Geotechnical Engineering.

[9] Das, B. M. (2015). *Principles of Geotechnical Engineering* (8th ed.). Cengage Learning.

[10] Ishihara, K. (1996). *Soil Behavior in Earthquake Geotechnics*. Oxford University Press.

[11] Moffat, R., & Fannin, R. J. (2006). Piping and internal erosion in cohesion less soils: Observations from laboratory model testing. *Canadian Geotechnical Journal*.

[12] ICOLD (International Commission on Large Dams). (2015). *Internal Erosion in Embankment Dams and Their Foundations*. Bulletin 164.

[13] Fell, R., MacGregor, P., Stapledon, D., Bell, G., & Foster, M. (2008). *Geotechnical Engineering of Dams* (2nd ed.).

[14] Pradel, D. (2010). *Soil Mechanics*. CRC Press.

[15] Mesri, G., & Feng, T. W. (1991). Secondary compression of peat with or without surcharge loading. *Journal of Geotechnical Engineering*.

[16] Mesri, G., & Godlewski, P. M. (1977). Time and stress compressibility interrelationship.

[17] Terzaghi, K., Peck, R. B., & Mesri, G. (1996). *Soil Mechanics in Engineering Practice* (3rd ed.). Wiley.

[18] Mesri, G., & Castro, A. (1987). The coefficient of secondary compression. *Journal of Geotechnical Engineering*.

[19] Lambs, T. W., & Whitman, R. V. (1969). *Soil Mechanics*. Wiley.

[20] Chen, Li, H. & Jiang, J. (2021). Numerical study on long-term consolidation settlement induced by tunneling in soft clay.

[21] Holtz, R. D., & Kovacs, W. D. (1981). *An Introduction to Geotechnical Engineering*. Prentice Hall.

[22] Craig, R. F. (2004). *Craig's Soil Mechanics* (7th ed.). Taylor & Francis.

[23] Mitchell, J. K., & Soga, K. (2005). *Fundamentals of Soil Behavior* (3rd ed.). Wiley.

[24] Leroueil, S. (2001). Natural slopes and cuts: movement and failure mechanisms. *Géotechnique*.

[25] Leroueil, S., & Hight, D. W. (2003). Behavior and properties of natural soils and soft rocks. In *Characterisation and Engineering Properties of Natural Soils*, Vol. 1. Sweet's & Zeitlinger.

[26] Gang Nia, Xu hen He, Haoding Xu, Shaoheng Dai, (2024). Tunneling-induced ground surface settlement: A comprehensive review with particular attention to artificial intelligence technologies.

[27] Moghaddasi, M.R., Noorian-Bidgoli, M., (2018). ICA-ANN, ANN and multiple regression models for prediction of surface settlement caused by tunneling.

[28] Martos, F., (1958). Concerning an approximate equation of the subsidence trough and its time factor. Int. Strata Control Cong. 191–205.

[29] Peck, R.B., (1969). Deep excavations and tunneling in soft ground. In: Proceedings of the 7th International Conference on Soil Mechanics and Foundation Engineering, pp. 225–290

[30] Ranken, W.J., (1987). Ground movement resulting from urban tunneling: predictions and effects.

[31] Attewell, P.B., Yeates, J., Selby, A.R., (1986). Soil Movement Induced by Tunneling and Their Effects on Pipelines and Structures.

[32] Chen, R.P., Zhang, P., Kang, X., Zhong, Z.Q., Liu, Y., Wu, H.N., (2019). Prediction of maximum surface settlement caused by earth pressure balance (EPB) shield tunneling with ANN methods.

[33] Su, J., Wang, Y., Nib, X., Shah, S., Yu, J., (2022). Prediction of Ground Surface Settlement by Shield Tunneling Using XGBoost and Bayesian Optimization, vol. 114. Engineering Applications of Artificial Intelligence.

[34] Zhang, L., Wu, X., Ji, W., AbouRizk, S.M., (2017). Intelligent approach to estimation of tunnel-induced ground settlement using wavelet packet and support vector machines.

[35] Zhang, P., Wu, H.N., Chen, R.P., Chan, T.H.T., (2020). Hybrid meta-heuristic and machine learning algorithms for tunneling-induced settlement prediction: a comparative study.

[36] Sagaseta, C., (1987). Analysis of undrained soil deformation due to ground loss.

[37] Verruijt, A., Booker, J.R., (1996). Surface settlements due to deformation of a tunnel in 759 an elastic half plane.

[38] Loganathan, B.N., Poulos, H.G., (1998). Analytical prediction for tunneling-induced ground movements in clays.

[39] Gonzaíez, C., Sagaseta, C., (2001). Patterns of soil deformations around tunnels. 524 Application to the extension of Madrid Metro.

[40] Burland, J.B. (1997). Assessment of risk of damage to buildings due to tunneling and excavation.

[41] Chiriotti E., Marchionni. V. and Grasso, P. (2000). Porto Light Metro System, Lines C, S and J. Interpretation of the results of the building condition survey and preliminary assessment of risk. Methodology for assessing the tunneling induced risks on buildings along the tunnel alignment.

[42] Chiriotti, E. & Grasso, P. (2001). Porto Light Metro System, Lines C, S and J. Compendium to the methodology report on building risk assessment related to tunnel construction.

[43] Rankin, W.J. (1988). Ground movements resulting from urban tunneling: predictions and effects.

[44] Lazarus, D., & Jung, H.-I. (2018). Damage assessment and monitoring for buildings on the Elizabeth line.

[45] New B.M, O'Reilly M.P. (1991): Tunneling induced ground movements: predicting their magnitude and effects.

[46] Z. C. Moh, Daniel H. Ju and R. N. Hwang (1996): Ground movements around tunnels in soft ground.